Cape Peninsula
University of Technology

MIGRATION OF CHEMICALS THROUGH COATED PAPERBOARD FOR FOOD CONTACT PACKAGING

by

PAULINE SKILLINGTON

Thesis submitted in fulfilment of the requirements for the degree

Master of Technology: Chemistry

in

the Faculty of Applied Sciences

at

the Cape Peninsula University of Technology

Supervisor: Dr Francois Wewers

Co-supervisor: Dr Patrice C. Hartmann & Dr J. Christel Cronje

Cape Town

August 2014

CPUT copyright information

The thesis may not be published either in part (in scholarly, scientific or technical journals), or as a whole (as a monograph), unless permission has been obtained from the University

DECLARATION

I, Pauline Skillington, declare that the contents of this thesis represent my own unaided work, and that the thesis has not previously been submitted for academic examination towards any qualification. Furthermore, it represents my own opinions and not necessarily those of the Cape Peninsula University of Technology.

_____   _____

Signed   **Date**

ABSTRACT

Paperboard made from recycled fibres is being used more frequently in direct food packaging applications, in addition to its use as secondary and tertiary packaging. However, recent research has shown that there is a risk that harmful chemicals may migrate from the paperboard into the food. The simplest approach to reducing the migration of these contaminants is the use of barrier films. The barrier efficiencies of these various films can be examined by means of a migration test into a food simulant, followed by extraction in a suitable solvent. The extract can then be analysed by chromatographic techniques such as gas chromatography mass spectrometry (GC-MS) to determine the concentration of the specific contaminants. However on a production level, the availability of this type of highly specialised equipment is limited. A simple, cost effective method is needed to evaluate the barrier properties to specific chemical contaminants. The Heptane Vapour Transmission Rate (HVTR) test is a permeation test method for use at quality control level to determine barrier properties to the migration of organic vapours.

The first part of the study focussed on establishing a universal correlation between HVTR and specific migration of diisobutyl phthalate (DiBP), dibutyl phthalate (DBP) and diethylhexyl phthalate (DEHP) that would be applicable to any type of functional barrier. However, experimental data demonstrated this was not possible as the correlation factor linking HVTR to specific migration was largely dependent on the type and morphology of the coating considered. The initial objective of the study was reconsidered in favour of building individual models specific to the nature of the coating and substrate considered. A correlation between HVTR and specific migration of DiBP, DBP and DEHP for a polyvinylidene chloride (PVDC) barrier polymer was constructed by varying the applied coating weight. The vapour transport mechanism for the HVTR test and the specific migration test were found to differ, showing that a direct correlation between HVTR and the specific migration was again not possible. However, an indirect correlation could be made. The HVTR method gives an indication of film integrity, whereas the coating weight could be used as an indicator of the specific migration. The correlation between the coating weight and the specific migration yielded an equation that can be used to calculate the specific migration through the PVDC barrier polymer, provided the quantity of the chemical contaminant originally present in the paperboard was known. This equation was specific to the type of barrier polymer, the specific chemical contaminant as well as the intended shelf-life of the food product to be packaged in the paperboard.

ACKNOWLEDGEMENTS

TABLE OF CONTENTS

LIST OF FIGURES

CHAPTER 6: THE CORRELATION BETWEEN HVTR AND SPECIFIC MIGRATION FOR A SPECIFIC BARRIER POLYMER

LIST OF TABLES

CHAPTER 6: THE CORRELATION BETWEEN HVTR AND SPECIFIC MIGRATION FOR A SPECIFIC BARRIER POLYMER

ABBREVIATIONS

ASE	*Accelerated solvent extractor*
BfR	*The German Federal Institute for Risk Assessment*
CEPI	*Confederation of European Paper Industries*
DAD	*Diode array detector*
DBP	*Di-n-butyl phthalate*
DEHP	*Bis (2-ethylhexyl) phthalate*
DiBP	*Di-isobutyl phthalate*
DiPN	*Diisopropylnaphthalene*
EU	*European Union*
EVOH	*Ethylene vinyl alcohol*
FAO	*Food and Agriculture Organisation of the United Nations*
FID	*Flame-ionisation detector*
GC	*Gas chromatography*
HDPE	*High density polyethylene*
HPLC	*High pressure liquid chromatography*
HTP	*Hydrogenated terphenyl*
HVTR	*Heptane Vapour Transmission rate*
ISQ	*Single Quadrapole*
JECFA	*Joint FAO/WHO Expert Committee on Food Additives*
LOD	*Limit of detection*
LOQ	*Limit of quantification*
MOAH	*Mineral oil aromatic hydrocarbon*

MOSH	*Mineral oil saturated hydrocarbon*
MS	*Mass spectrometer*
OML	*Overall Migration Limit*
OPP	*Orientated polypropylene*
PA	*Polyamide*
PCB	*Polychlorinated biphenyls*
PE	*Polyethylene*
PET	*Polyethylene terephthalate*
PP	*Polypropylene*
QMA	*Quantity of Material*
%RH	*Relative humidity*
SiOx	*Silicon Oxide*
SML	*Specific Migration Limit*
Tg	*Glass transition temperature*
UV	*Ultra violet*
WHO	*World Health Organisation*

CHAPTER 1

INTRODUCTION

1.1   Introduction

Paperboard can be defined as a sheet of cellulose fibres formed on a fine screen from a water suspension.[1] Paperboard is light in weight, easily cut and formed and has high strength that makes it advantageous for use in the packaging industry. Paperboard packaging is made from a renewable material, wood, which is its main advantage over other types of packaging materials. In addition, paperboard can be recycled up to seven times and modern paperboard manufacturing processes are operating on a closed-loop system, requiring no external energy input.[2] Paperboard packaging forms part of our everyday lives, with products such as pharmaceuticals, toothpaste, cereal, rice, flour and fast food, to name a few, making use of paperboard packaging.

The South African Pulp and Paper Industry is a major contributor to the South African economy, bolstering the economy by R 4.5 billion in 2011. In 2012, almost 2.5 million tons of paper-based products were produced in South Africa, with paperboard for packaging applications accounting for 50% of the total production. The raw material for the production of paper-based products is composed of virgin fibre as well as recycled fibre. In 2012, 1.1 million tons of recycled fibre was used in the production of paper-based products in South Africa, the majority which is most likely used in the production of newsprint and paperboard packaging materials.[3, 4]

The increased use of recycled fibre in the production of paperboard packaging materials has prompted the food packaging industry to investigate the suitability of recycled paperboard for use in food packaging applications. The origin of recycled fibre may vary i.e. newsprint, corrugated containers, cartons, and as such the possible sources of contamination (e.g. printing inks, adhesives, waxes, fluorescent whitening agents, sizing agents and biocides) are vast. Chemical contaminants present in the recycled paperboard can migrate from the paperboard into the food, thereby constituting a health concern for the end-consumer.

As a result, regulatory bodies impose stringent rules on packaging materials, with specific migration limits (SML) set for a vast range of potentially hazardous chemicals that may be present in recycled paperboard.[5, 6, 7]

The most effective strategy proposed to impede the migration of chemical contaminants is the use of functional barriers either in the form of an inner liner or as a barrier coating on the

inner side of the paperboard. The efficiency of these functional barriers can be assessed using a conventional migration test which involves the use of a food simulant and the quantification of the migration of organic chemical contaminants into the simulant by chromatographic techniques. Alternative techniques will be employed to quantify inorganic contaminants.

Implementation of migration testing at quality control level during the manufacture of paperboard is not a practical option. The migration test involves placing the paperboard into contact with a suitable food simulant for a specific time period and at a specific temperature. Thereafter, the food simulant is extracted in a suitable solvent and the extract quantified by chromatographic techniques to determine the concentration of the chemical contaminants that have migrated from the paperboard into the food simulant. The migration test is time consuming and the chromatographic equipment required for quantification of specific migration limits (SML's) are very costly and require a high level of operator expertise.

A simplified permeation test method that simulates the general migration behaviour of organic vapours through the functional barriers can be used as an indication of the barrier efficiency. There is however no correlation between the results of the permeation method and actual migration levels of specific contaminants.

This study aims to correlate the results of a permeation method to the actual migration levels of specific organic chemical contaminants. The permeation method, defined by the heptane vapour transmission rate (HVTR) is a simple, rapid method that can be implemented in a quality control laboratory with minimal start-up costs and level of operator expertise. The method is based on the mass pickup of a suitable absorbent after being exposed to a saturated heptane environment for a predefined time period. The HVTR and the actual specific migration levels will be plotted against each other to determine whether a simple correlation between the two variables is possible.

1.2 Objective

To determine whether a correlation exists between the HVTR and the actual migration levels of specific organic contaminants for a number of barrier films of varying efficiency.

1.3   Layout of the thesis

Chapter 1 of this thesis contains a short introduction to the initiation of the study as well as the objective. Chapter 2 outlines the theoretical principles and related studies in literature, with specific focus being given to diffusional mechanisms and migration testing. Chapter 3 outlines all the materials used and experimental procedures. Chapters 4 to 6 detail the construction of the correlation between HVTR and specific migration. Chapter 7 will summarise the conclusions of the study and recommendations for future work.

CHAPTER 2

THEORETICAL BACKGROUND

2.1 Introduction

A growing area of research in the paperboard packaging industry is the suitability of recycled paperboard for use in food packaging. However, using recycled fibres comes with new challenges, such as controlling potential contamination of the packaging by harmful chemicals introduced by using pre- and post-consumer waste. Numerous studies have revealed the migration of various contaminants such as phthalates[8], benzophenones[9], diisopropyl naphthalenes[10], Michlers ketones and aromatic amines[11], amongst others. Recent work[12] published at the Official Food Control Authority of the Canton showed that relatively high levels of mineral oils may migrate from packaging manufactured from recycled fibre into the food it contains, via either direct or indirect contact. The mineral oils detected contain both the mineral oil saturated hydrocarbon (MOSH) and mineral oil aromatic hydrocarbon (MOAH) fractions. This has raised a new concern in the food packaging industry as the toxicity of the aromatic fraction is currently unknown.

2.2 Sources of contaminants

The origin of the raw materials used in the production of recycled paperboard varies significantly and as such will contain a wide variety of possible contaminants such as printing inks, adhesives, waxes, fluorescent whitening agents, sizing agents and biocides. The most important contributor to low molecular weight contaminants in recycled paperboard is recovered printed material, of which phthalates and benzophenones are most commonly reported. Carbonless copy paper and thermal copy papers are next on the list, contributing to contamination with polychlorinated biphenyls (PCB), diisopropylnaphthalenes (DiPN) and hydrogenated terphenyl (HTP) isomer mixtures.[13]

Table 2.1: *Contaminants present in recovered paper and board packaging.* [14, 15, 16]

Contaminant	Limit Food (mg/kg)	Limit Paperboard	Source	Contaminant	Limit Food (mg/kg)	Limit Paperboard	Source
Cadmium [a]	-	0.5 mg/kg	Inks	Sum of DBP and DiBP [b] ([ ] = limit in baby food)	1.0 [0.5]	0.17 [0.08] mg/dm^2	-
Lead [a]	-	3.0 mg/kg	Inks	Di(2-ethylhexyl)phthalate (DEHP) [b]	1.5	0.25 mg/dm^2	Adhesive plasticiser Defoamers
Mercury [a]	-	0.3 mg/kg	Inks	Benzylbutylphthalate (BBP) [b]	30	5.0 mg/dm^2	
Pentachlorophenol	-	0.15 mg/kg	Biocide	Diisononylphthalate (DiNP) [b]	9.0	1.5 mg/dm^2	Hot melt adhesives
Azo colourants (sum of listed aromatic amines) [a,b]	-	0.1 mg/kg	-	Diisodecylphthalate (DiDP) [b]	9.0	1.5 mg/dm^2	-
Primary aromatic amines (PAAs) [a]	< 0.01		Overprint varnish Polyurethane adhesives	4,4-bis(diethylamino) benzophenone (DEAB) [a, b]	0.01	0.0016 mg/dm^2	UV ink photointiator
Dyes and colourants [a]	-	No bleeding	-	Michler's Ketone [a,b]	0.01	0.0016 mg/dm^2	UV ink photointiator
Fluorescent whitening agents (FWAs) [a]	-	No bleeding	-	Benzophenone (BP) [b]	0.6	0.1 mg/dm^2	UV ink photointiator, Pigment wetting agent
Formaldehyde	-	1.0 mg/dm^2	Dry strength resins, Crosslinkers	Sum: BP + Hydroxybenzophenone + 4-methylbenzophenone	0.6	0.1 mg/dm^2	-
Polycyclic aromatic hydrocarbons (sum of listed PAHs) [b]	0.01	0.0016 mg/dm^2	-	Diisopropylnaphthalene (DiPN) [b]	-	As low as possible	Carbonless and thermal copy paper
Dibutylphthalate (DBP) [b]	0.3	0.05 mg/dm^2	Plasticiser, adhesives, printing inks	Bisphenol A [a/ b]	0.6	0.1 mg/dm^2	Epoxy-phenolic resins as printing ink binder
Diisobutylphthalate (DiBP) [b] ([ ] = limit in baby food)	1.0 [0.5]	0.17 [0.08] mg/dm^2	Adhesive plasticiser				

[a] *Testing required only if paper or paperboard is in direct contact with moist or fatty foodstuff;* [b] *Found only in recovered paper / board, testing not required for 100% virgin products; - indicates no data was available.*

2.3 Food packaging regulations

The legal migration limits for different chemical contaminants migrating from the packaging into the food are expressed by the specific migration limit (SML) and the overall migration limit (OML). The SML is the tolerable daily intake of a specific compound expressed in (mg/kg body weight/day). These values are obtained assuming an average body weight of 60 kg and the consumption of 1 kg of food per day. The OML is the sum of the SML's of all compounds of concern and is currently set at 60 mg/kg of food.[17] The SML values are laid down in a number of regulatory documentation. The European Directive 10/2011[18] defines a positive list system for application to plastic manufacture. The German Federal Institute for Risk Assessment (BfR)[14], The Confederation of European Paper Industries (CEPI)[15] and Regulation (EC) 1935/2004 outlines the substances that can be used in the production of paperboard.

If it is assumed that complete migration of chemical contaminants from the paperboard into the food takes place, it is then possible to convert the SML's in food to a total quantity of chemical contaminant in paperboard. The standard packaging-to-food ratio in European Union (EU) risk assessments of paperboard packaging is 6 dm^2 paperboard in direct contact with 1 kg food.[18] The maximum permitted content of a specific contaminant in 1 dm^2 paperboard may be calculated from Equation 2.1.

$$QMA(mg/dm^2) = \frac{SML(mg/kg)}{6} = SML(mg/kg) \times 0.167 \qquad \textit{Equation 2.1}$$

Where *QMA* is the quantity of contaminant and is the maximum permitted quantity of a contaminant in the finished material.

2.4 The Theory of Permeation

2.4.1 The principles of permeation

The permeability of a polymer film can be described as the amount of penetrant, either gas or vapour, that will be transmitted through polymer film under the influence of a pressure or concentration gradient. The primary mechanism of gas or vapour transfer through a polymer film from a reservoir of high concentration to a reservoir of low concentration is by a process of activated diffusion. The mechanism is depicted graphically in Figure 2.1. A polymer film

with a thickness, *l*, separates two reservoirs with different partial pressures and concentrations of the diffusing gas or vapour where $p_1 > p_2$ and $c_1 > c_2$. The gas or vapour will dissolve into the polymer, diffuse through the film under the influence of the concentration gradient and evaporate at the other side of the film.[19, 20]
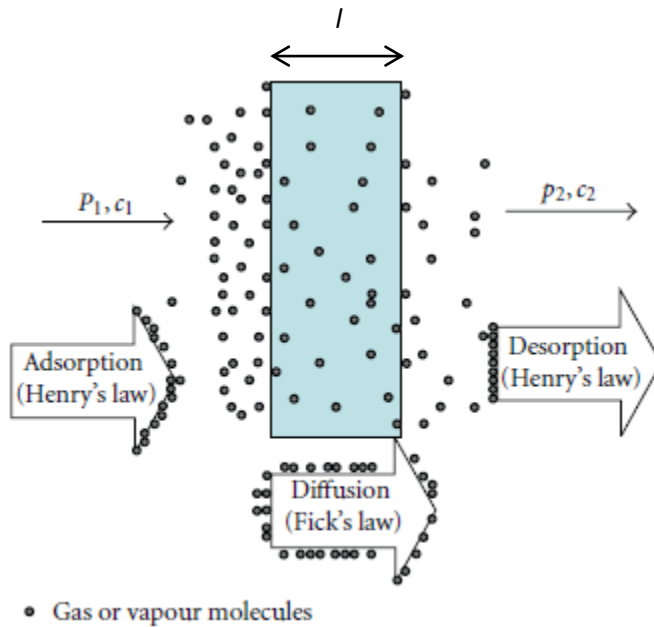
Figure 2.1: *General mechanism of gas or vapour permeation through a plastic film.*[20]

2.4.1.1 The permeability coefficient, P

The ease with which the gas or vapour is transported through a polymer film is described by the permeability coefficient, *P*, and is the product of the diffusion coefficient, *D*, and solubility coefficient, *S*.

$$P = D \times S$$
<div align="right">*Equation 2.2*</div>

2.4.1.2 The diffusion coefficient, D

The diffusion coefficient describes how fast the penetrant is transported through the barrier film and is best described by Fick's First Law. The film shown in Figure 2.1 has a specific thickness, *l,* and an area, *A*. The total amount of a penetrant, *Q*, that passes through the film during the time, *t*, is defined as the diffusional flux, *J*. Fick's First Law correlates the diffusional flux to the concentration gradient, *Δc*, across the polymer film by means of the

diffusion coefficient, D. This law is only applicable in the steady state, where the flux is constant and the concentration of the penetrant remains constant.[21]

$$J = \frac{Q}{At} = -D\Delta c$$

Equation 2.3

However, in the non-steady state, Fick's Second Law applies where the concentration of the penetrant is a function of its position, x, within the film and time, t.[21]

$$\frac{dC}{dt} = D\frac{d^2C}{dx^2}$$

Equation 2.4

The diffusion of a penetrant is linked to the physical properties of the polymer network and the interaction between the penetrant and the polymer. As such, diffusion can be classified according to the penetrant diffusion rate, R_{diff}, and the polymer relaxation rate, R_{relax}, as Fickian and Non-Fickian (Table 2.2). Fickian diffusion is most commonly observed in rubbery polymers, where the temperature, T, of the polymer is above than the glass transition temperature of the polymer, Tg (i.e. T > Tg). The high mobility of the polymer chains enables redistribution of the free-volume holes required for diffusion of the penetrant to occur. Non-Fickian diffusion is most commonly observed in glassy polymers, where the temperature, T, of the polymer is below the glass transition temperature of the polymer, Tg (T < Tg). The polymer chains are not mobile enough to enable sufficient redistribution of the free-volume holes required for diffusion of the penetrant to occur.[22]

The amount of penetrant adsorbed per unit area of polymer film at time t is expressed by

$$M_t = kt^n$$

Equation 2.5

where k is a mass transfer constant and n a parameter related to the diffusion mechanism, the value of which lies between ½ and 1. This equation can be used to describe the

diffusional behaviour of any polymer-penetrant system regardless of the temperature or the penetrant activity.[22]

Table 2.2: *Characteristics of diffusion classes.*[22]

Class	Diffusion rate relationship	Occurrence	n
Fickian, Case I	$R_{diff} << R_{relax}$	Above Tg	½
Non-Fickian, Case II	$R_{diff} >> R_{relax}$	Below Tg	1
Non-Fickian, Anomolous	$R_{diff} = R_{relax}$	Below Tg	½ < n < 1

2.4.1.3 The solubility coefficient, S

The solubility coefficient describes how much penetrant is adsorbed or dissolved in the polymer film. Adsorption can occur by a number of different modes as illustrated in Figure 2.2. The simplest case is the Henry adsorption mode where the concentration, *C*, of the penetrant adsorbed in the polymer film is proportional to the partial pressure, *p* of the penetrant.

$$C = S \times p$$ *Equation 2.6*

This mode of adsorption is applicable to ideal gases, where no interaction takes place between the penetrant and the polymer.

The Langmuir-Mode adsorption is characterised by polymer-penetrant interactions. The penetrant molecules occupy specific sites within the polymer such as microvoids and inorganic fillers. The Dual-Mode adsorption is used to describe the behaviour of low-activity gases in glassy polymers. It proposes the existence of two populations of penetrant molecules, the behaviour of which can be described by a combination of the Henry- and Langmuir-Mode adsorption. The Flory-Huggins Mode adsorption can be applied to hydrophobic polymer systems where the interaction between the penetrant molecules is greater than the polymer-penetrant interactions. The Brunauer, Emmet and Teller (BET) mode adsorption is used to describe the adsorption of water in hydrophilic systems. It is a

combination of the Langmuir and the Flory-Huggins adsorption modes where penetrant-polymer and penetrant-penetrant interactions dominate respectively.[21, 23]
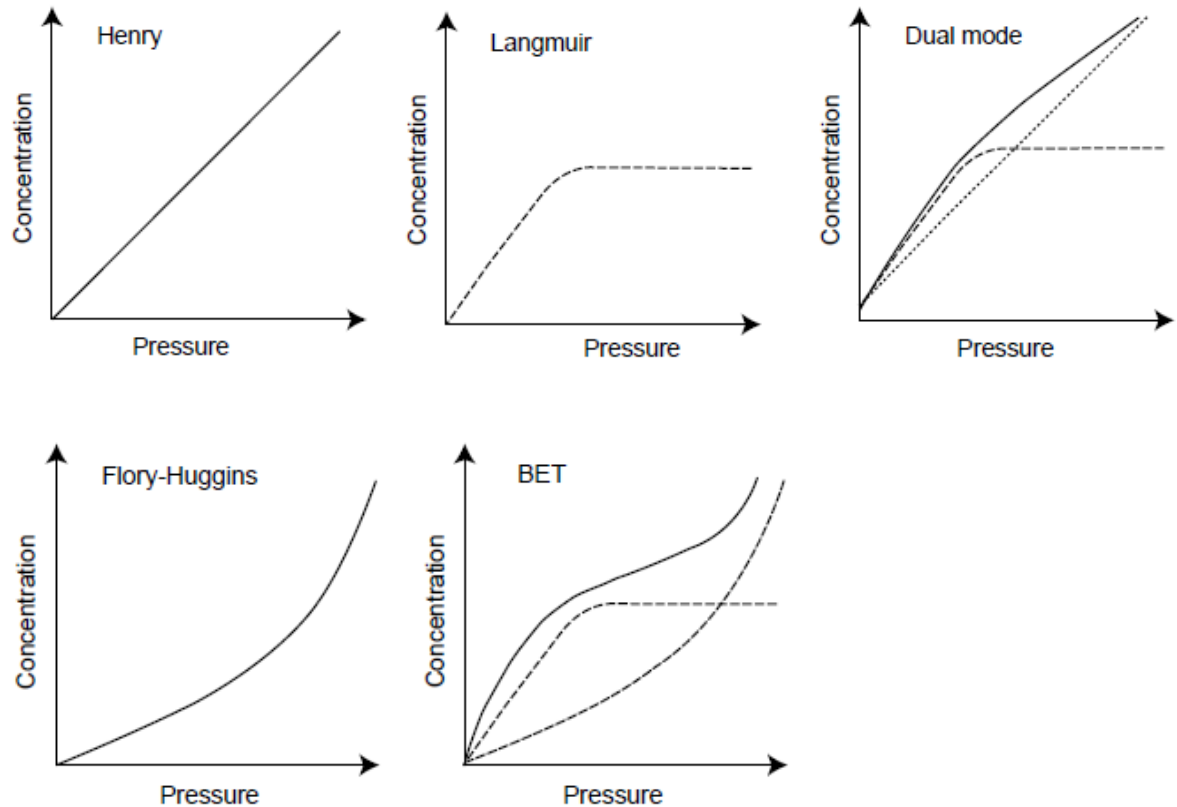
Figure 2.2: *Typical isotherm plots of adsorbed concentration vs. vapour pressure.[21]*

2.4.2 Diffusion kinetics

Fick's first law states that the diffusional flux, *J*, of a penetrant is directly related to the diffusion coefficient, *D* and the concentration gradient, *Δc*. When the concentration gradient across the membrane remains constant, the diffusional flux will also remain constant. A plot of the amount of penetrant, *Q*, migrating across the membrane against time, *t*, will yield a straight line. This would typically occur when the diffusion takes place from a saturated environment.

However, when the penetrant is present within the membrane and is depleted over time, the concentration gradient is reduced and subsequently the diffusional flux. A plot of the amount of penetrant migrating from the membrane against time would initially be a straight line, with the gradient decreasing to a point where the amount of penetrant that migrates does not

change with time.[21, 24] This would typically be observed in a migration experiment from a packaging material into a food or food simulant.
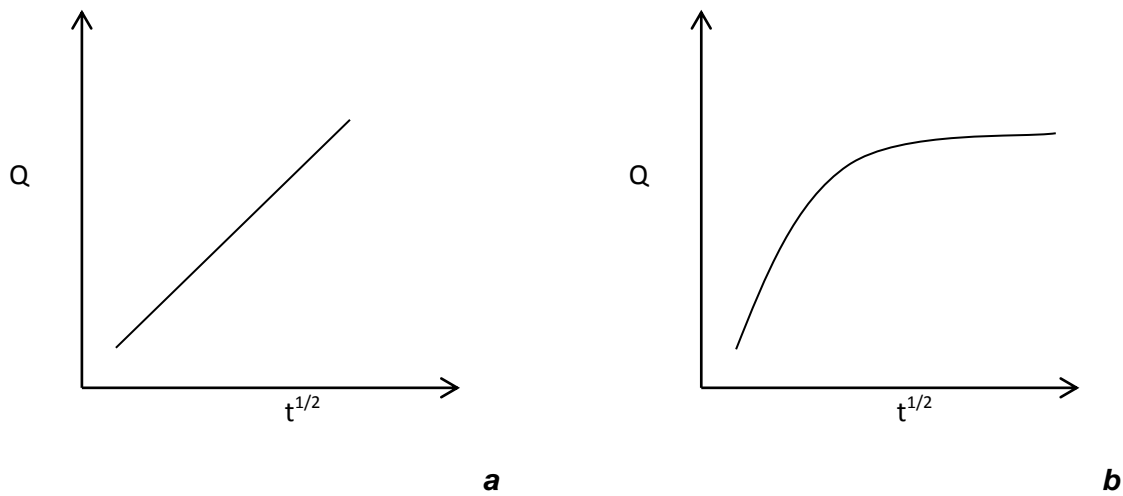
Figure 2.3: *Relationship between penetrant transfer through a membrane over time with (a) constant concentration gradient and (b) decreasing concentration gradient.*

2.4.3   Mechanism of mass transfer in polymers

Migration of organic vapour molecules through a polymeric film is best described by the free volume theory.[25] The total volume of a polymer film can be divided into the occupied volume and the free volume. The free volume is continuously redistributed throughout the barrier film as a result of the mobility of the polymer chains. However, a state will exist where the free volume cannot be redistributed without overcoming an activation energy barrier. For this reason, the free volume is divided into two types i.e. the interstitial and hole free volume. The interstitial free volume requires large redistribution energy and does not enable molecular transport through the film. The hole free volume is easily redistributed and is presumed to control molecular transport.

The migration or diffusion of organic vapour molecules through the film can be seen as a series of "jumps" of the molecular units between the free volume holes. The rate of migration is proportional to the probability of finding a free volume hole that is large enough to accommodate the molecular unit adjacent to its current position. The probability of finding a free volume hole is governed by the temperature of the material relative to the glass transition temperature, Tg, of the polymer. Above the Tg, the polymer chains have sufficient mobility, allowing volume relaxation to occur within commonly referenced time frames.

11

However, as the temperature is reduced to below the Tg, the movement of the polymer chains becomes constrained, trapping additional hole free volume within the film and prevents volume relaxation from reaching equilibrium. This limits the redistribution of the free volume and the additional "trapped" free volume does not contribute to the vacant space available for penetrant transport through the film. The free volume theory predicts that the diffusion coefficient of a penetrant is dependent on the amount of additional trapped free–volume, where the diffusion rate below the Tg is inversely proportional to the amount of trapped free volume.[25]
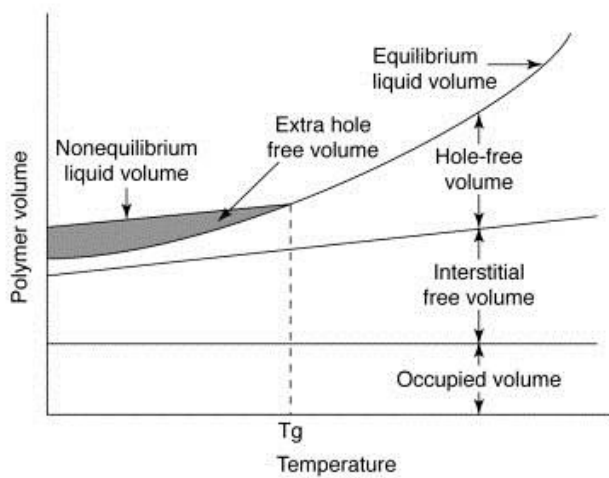
Figure 2.4: Characteristics of the volume of a polymer above and below the glass transition temperature (Tg).[25]

2.4.4   Mechanisms of penetrant transfer through thin polymer films

In a compressive review article by Chatham[26], the movement of penetrant molecules through thin barrier films applied to a polymer surface was described to occur by two pathways, with the dependency of the penetrant transmission rate on the coating thickness being very different for the two mechanisms. The studies he reviewed evaluated the permeability of non-condensable gases such as oxygen. The mechanisms described below may differ slightly when applied to condensable vapours such as water and organic vapours due to the increased interaction that may occur between the penetrant, substrate and/or barrier film.

2.4.4.1 Diffusive flow by the solution-diffusion mechanism

The diffusive flow of a penetrant, *i*, through the substrate and the barrier film is described by:

$$\frac{1}{\rho_{i,\mathrm{T}}} = \frac{\tau_T}{P_{i,T}} = \frac{\tau_s}{P_{i,s}} + \frac{\tau_c}{P_{i,c}}$$

Equation 2.7

where $\rho_{i,\mathrm{T}}$ is the total permeation rate of penetrant, $P_{i,T}$ is the apparent permeability of the penetrant in the whole structure, τ_T is the total thickness ($\tau_s + \tau_c$) and $P_{i,s}$ and $P_{i,c}$ are the permeabilities of the penetrant in the substrate and the coating, respectively. Therefore, according to this mechanism, the total permeation rate of the penetrant will decrease as the thickness of the barrier film is increased.[26]

2.4.4.2 Flow through defects such as pinholes (Defect Model)

Prins and Hermans[26, 27] developed an expression for the flux, F_i, of a penetrant, *i*, through defects such as pinholes in a metallised polymer. They applied the steady state diffusion equation and obtained,

$$Fi \approx \frac{Di}{\tau_s}(c_o - c_1)\Theta(1+1.18\lambda)$$

Equation 2.8

where Di is the diffusion coefficient of the penetrant in the polymer, τ_s is the polymer thickness, Θ is the fraction of the surface left uncovered by the defects, c_o and c_1 are the concentrations of the penetrant on either side of the barrier film and λ is the ratio of the film thickness to the radii of the defects. This mechanism predicts that the flux is directly proportional to the diffusion coefficient of the polymer, the concentration gradient as well as the fraction of the surface left uncovered by defects such as pinholes and is independent of the barrier film thickness.[26]

2.4.5 Mechanism of mass transfer in paperboard

The movement of organic vapours through a paperboard matrix is much more complex than through polymer films. The migrants are already present within the paperboard matrix. In addition, the paperboard can be composed of virgin or recycled fibres, additives such as fillers, sizing agents, wet strength resins and pigment or polymer coatings. These additives contain active sites onto which migrants can be adsorbed.

The mechanism of mass transport through the paperboard can be described as a continuous process of desorption and adsorption until a thermodynamic equilibrium is reached. Zulch and Piringer[28] described diffusion in paperboard using a two-layer approach. Paperboard can be considered as two layers B_1 and B_2 with thickness $d_{B1} >>> d_{B2}$.
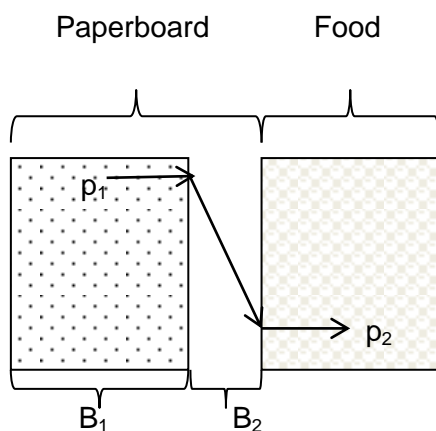
Figure 2.5: *Two-layer diffusion approach used to describe the movement of migrants present in paperboard.*

Layer B_1 contains the main part of the migrant which permeates through the thin layer B_2 at the interface to the food or food simulant. Diffusion in B_2 normally occurs at a slower rate than in B_1. Therefore, the rate of mass transfer from the paperboard to the food or food simulant is determined by the diffusion through the surface layer B_2 and is proportional to the ratio of the diffusion coefficient (D_{B2}) and the thickness (d_{B2}) of this layer. The desorption rate of the migrant from the surface into the food or food simulant is the rate determining step and is dependent on the interaction strength between the board surface and the migrant. This is described by the mass transfer coefficient, *k*. Due to the complex nature of the interactions occurring within the paperboard matrix, diffusion will either comply with Fick's First Law (mass transfer is proportional to time) or Fick's Second Law (mass transfer is proportional to

the square root of time) depending on the specific chemical contaminant as well as the environmental conditions.

A one-layer approach can be used to describe diffusion behaviour of migrants with low polarity and molecular weights below 350 $g.mol^{-1}$ through paperboard of high porosity and grammage, at high temperatures and high humidity. This is due to the increased desorption rate in B_2, which leads to diffusion coefficient in B_2 approaching the same magnitude as the diffusion coefficient in B_1, where $D_{B1} = D_{B2} = D_B$. Further work by Hauder *et al.*[29] and Hellen *et al.*[30] confirmed that differentiation between the diffusion rates in B_1 and B_2 is unnecessary at the above mentioned conditions.

2.5   The migration test setup

2.5.1   Single-sided

This is the more realistic approach to testing the migration of substances between two media. In this setup, a migration cell is used, where the sample is fixed between a flat flange of a beaker and lid such that only one side of the paperboard is in contact with the food or food simulant. The food or food simulant is added into the cell via an opening in the lid.[17]

Migration cell with a food simulant in contact with one side of the sample

Paperboard sample
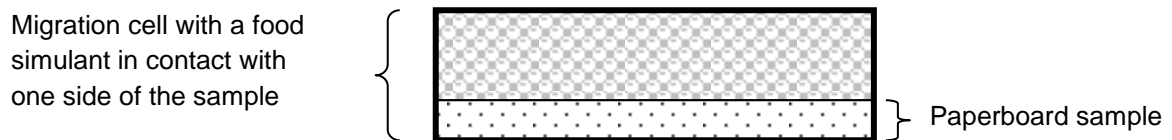
Figure 2.6: *Single-sided migration test setup.*

2.5.2   Total Immersion

This is the easiest manner of testing. In this setup, both surfaces of the sample are in contact with the simulant and migration occurs from both sides. The partitioning equilibrium is therefore reached at a faster rate in comparison to the single-sided method, but yields the same total migration.[17]

Migration cell with a food simulant in contact with both sides of the sample

Paperboard sample
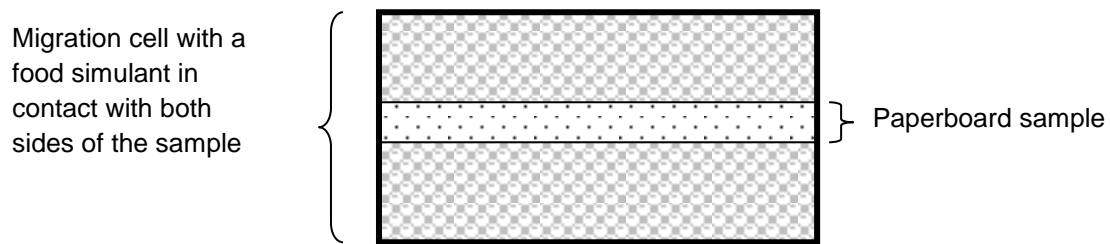
Figure 2.7: *Total immersion migration test setup.*

2.6 Factors affecting the migration

Several factors that may determine the level and rate of chemical contaminant migration from paperboard packaging into food or food simulant have been suggested in numerous sources of literature. These include:

2.6.1 Type of contact between paperboard and food

Paperboard used as the primary packaging will have direct contact with the food packaged within. The paperboard can also be used as secondary packaging, where the food and the paperboard are separated by a plastic film liner, or as the tertiary packaging as in the case of a corrugated box for transport of the product; in which case the contact is indirect. It has been shown that migration rates are higher when there is direct contact between the paperboard and the food.[9] Boccacci-Mariani *et al.*[10] showed that in the case of direct contact, factors such as contact time, food characteristics and contaminant concentration in the paperboard also have an influence on the migration, where only contact time plays a role in indirect contact migration.

2.6.2 The food or food simulant

Foods can be classified as aqueous, acidic, alcoholic, fatty or dry. The fat content and the specific surface area of the food impact the degree and rate of migration. Usually, greater migration is observed into food with high fat content due to the high fat solubility of a large majority of chemical contaminants.[7, 9, 10] The particle size of the food also impacts migration. Foods with small particle size will have a large specific surface area which results in an increased adsorption rate of volatile compounds. When selecting a food simulant, in the case of dry foods, the simulant should be a solid adsorbent that mimics the contact with dry foods. For example, Tenax® (modified polyethylene oxide) is defined in Directive 10/2011[18] as a suitable simulant for fatty dry foods tested at high temperatures.

Table 2.3: *Classification of foods and the types of chemical migration that they are likely to elicit.[31]*

Nature of food in contact	Nature of chemicals most likely to migrate
Aqueous, Acidic, Low alcoholic beverages	Polar organic chemicals, salts, heavy metals
Fatty foods, distilled spirits	Non-polar, lipophilic organic substances
Dry foods	Low molecular weight, volatile substances

2.6.3   The type of paper (thickness, porosity, lignin content and recycled fibre content)

The thickness and grammage of the paperboard have been found to play a significant role in the migration rate. Fast migration is observed for paperboard of low grammage and thickness as there is a shorter pathway for the chemical contaminant to travel from the bulk of the paperboard to reach the surface.[32] Paperboard of high porosity also shows greater migration rates as the pathway to the paperboard surface is less restricted as in the case of a denser paperboard sample.

The recycled fibre content does not appear to influence the migration rate[13, 32, 33], however as the recycled fibre content is increased, more chemical contaminants will be available to migrate from the paperboard to the food.[32]

The extent to which a chemical contaminant is retained within the paperboard is related to the interaction between the chemical contaminant and the fibre surface. The fibre surface has an overall negative charge due to the carboxyl groups from the carbohydrates and the hydroxyl groups from the lignins. Electron dense chemical contaminants such as naphthalene tend to be repelled by the fibre surface and are strongly partitioned into the gas phase.[33] Thus greater migration from the paperboard into the food is observed. The converse applies to more polar chemical contaminants.

2.6.4   The chemical nature of the chemical contaminant (volatility, polarity, molecular weight and structure)

The affinity of the chemical contaminant for the different food types (see Table 2.3) as well as the packaging material determines the extent of migration that will be observed. The boiling

point or volatility as well as the polarity and affinity with the fibre surface determines the partitioning behaviour of the chemical contaminant between the paperboard and air during the gas-phase migration.[33] For example, Triantafyllou *et al.*[34] showed that even though acetophenone has a very high volatility, its migration is much less than anticipated due to its high affinity with the cellulose fibres. The molecular size and weight of the chemical contaminants also has an influence on its tendency to migrate from the packaging into the food or food simulant.[33] Small, low molecular weight chemical compounds tend to migrate to a greater extent than bulky high molecular weight chemical compounds. This is due to the greater diffusivity of the smaller molecules.[35]

2.6.5 Time and temperature of contact

The amount of chemical contaminant that migrates from paperboard into the food is determined by the contact time. The longer the contact time, the greater the concentration of the chemical contaminant in the food. The migration from paperboard is very rapid. Castle[13] observed that the maximum migration plateau of methyl stearate, which was the largest molecule evaluated in the study and the slowest to migrate, was reached after 10 days at 20°C.

The effect of temperature on permeability and diffusion can be described by the Arrhenius equation.[36]

$$P = P_o \exp^{(-\frac{Ep}{RT})} \qquad\qquad\qquad \textit{Equation 2.9}$$

$$D = D_o \exp^{(-\frac{Ed}{RT})} \qquad\qquad\qquad \textit{Equation 2.10}$$

where P and D are the permeability and diffusion coefficients respectively, P_o and D_o are pre-exponential factors, E_p and E_d are the activation energy for permeation and diffusion respectively (J.mol^{-1}), R is the gas constant (J.mol^{-1}.K^{-1}) and T is temperature (K). Temperature also has an impact on the maximum migration plateau, with equilibrium being reached faster at higher temperatures. The partition coefficient of the chemical contaminant is increased at higher temperatures. This reduces the affinity of the chemical contaminant for the paperboard. The net result is increased migration of the chemical contaminant from the paperboard to the food or food simulant.[13, 33, 34]

2.7 Migration Studies of Possible Chemical Contaminants in Paperboard

2.7.1 The "Real-Time" Absolute Test Method

The "real-time" absolute test method mimics the actual storage conditions of paperboard packaged food and measures the migration of potentially hazardous chemical contaminants from the paperboard into the food. Vapour-phase migration of potential chemical contaminants such as mineral oils, benzophenones, ketones, phthalates and naphthalenes from paperboard into food has been reported.

2.7.1.1 Mineral Oil

Biedermann and Grob[12] reported the presence and composition of mineral oils in recycled paperboard as well as their migration into food. In the study, the concentrations of the mineral oil saturated hydrocarbon (MOSH) and mineral oil aromatic hydrocarbon (MOAH) fractions were determined by online HPLC-GC-FID in an ethanol:hexane (50:50) extract from paperboard samples and in hexane extract from rice samples. It was shown that the high levels of MOSH and MOAH fractions observed in the paperboard samples originate from printing inks used for newsprint, as newsprint is extensively used as a fibre source for the manufacture of recycled paperboard. The large amount of mineral oil (19 mg/kg) that migrated into the rice was confirmed not to originate from the printing ink, varnish and adhesive used in the production of the rice packaging.

Vollmer *et al.*[37] surveyed the German paperboard packaging market in an effort to set up a database for the BfR to prepare recommendations on the use of recycled fibres and for the German government to draft new regulations. The study comprised the analysis of one hundred and nineteen different dry food samples. The paperboard, food and internal bag (if present) were tested for the presence of mineral oils. The same analysis protocol as Biedermann and Grob[12] was used and found that the concentration of mineral oil migrating from the paperboard into dry foods exceeds the 0.6 mg/kg limit established by the JECFA evaluation[38] by a factor of 10-100. It was also found that 10-20% of the migrating mineral oil is the MOAH component, the toxicity of which remains controversial and still to be determined.

2.7.1.2 Benzophenone

Pastorelli *et al.*[39] studied the migration of benzophenones from UV-cured printed paperboard used as a secondary packaging for cakes. Extraction in acetonitrile and analysis by HPLC showed significant levels of benzophenone in forty different cake samples, despite the presence of a polypropylene inner barrier film.

Anderson and Castle[9] also published a study concerning the migration of benzophenones from paperboard packaging into food. Three hundred and fifty samples of paperboard packaged food purchased from a retail store were analysed. These included frozen, refrigerated and shelf-stable foods. The levels of benzophenone in both the paperboard and the food were determined by solvent extraction and analysis by GC-MS. Benzophenone migration was found to be influenced by a number of factors such as food fat content, paperboard grammage and density, and storage temperature.

2.7.1.3 Michlers Ketone

Castle *et al.*[11] conducted a two-phase study to establish the levels of Michlers Ketone in paperboard packaged samples sold in the United Kingdom as well as to evaluate the potential for migration into the packaged food. One hundred and seventy one paperboard packaged foods were purchased during the two-phase study and included frozen and shelf–stable foods as well as products for high-temperature applications e.g. microwaveable food packaging. Very low levels were observed in the paperboard via HPLC analysis and no detectable migration into the food was observed via GC-MS analysis.

2.7.1.4 Phthalates

Aurela *et al.*[8] studied the different types and levels of phthalates present in paperboard intended for sugar packaging. Twenty nine different paperboard samples were obtained from the manufacturer. Hexane extracts of the samples and analysis by GC-MS identified di-(2-ethylhexyl)phthalate (DEHP), dibutylphthalate (DBP) and diisobutylphthalate (DiBP) as the most common. Eighteen of the twenty nine samples showed phthalate levels exceeding 5 mg/kg, which far exceeds the set migration limits.[14, 15, 16, 18] The migration of these phthalates into sugar was also studied under normal conditions. Hexane extracts of the sugar samples were analysed by GC-MS. Approximately 74% migration of DiBP and 57% migration of DBP were reported, indicating significant migration from the paperboard into the sugar.

2.7.1.5 Naphthalenes

Boccacci-Mariani *et al.*[10] studied the migration of diisopropylnaphthalene (DIPN) from artificially contaminated paperboard samples into dry food (pasta, rice and flour). Direct and indirect contact migration tests were conducted over a number of time intervals up to 60 days at ambient temperature. The extent of migration was determined by GC-FID, with confirmation analysis via GC-MS. In the case of the direct contact experiments, it was found that the low migration levels observed were dependent on the contact time, whereas the indirect experiment showed that migration of DIPN is dependent on the characteristics of the

food, the DIPN concentration in the paperboard and the contact time. The greatest migration was observed for food with the highest fat content and specific surface area, the paperboard with the highest DIPN concentration and the longest contact time.

2.7.2 The Accelerated Absolute Test Method

Real-time migration testing is not practical in terms of quality control at the production level. As such, accelerated conditions for migration tests that correlate well with real-time migration tests are required. Currently, there are no standard conditions defined for paperboard testing. The accelerated conditions applied to plastics testing have been applied to paperboard testing using Tenax® as the food simulant for dry and fatty foods. Paperboard packaging is mostly applied to dry foods stored at room temperature, thus Test number OM2 as defined by Directive10/2011[18] is most applicable, where the migration test is carried out over 10 days at 40°C.

The migration test of paper and board using Tenax® as a simulant is described in DIN EN 14338[40] using the temperature and time conditions as specified in Directive 10/2011[18]. The test method was specifically designed for dry, non-fatty foodstuffs and baking applications. Tenax® is the commercial name for modified polyethylene oxide (MPPO). It is a porous polymer that is well suited to adsorb volatiles. Its thermal suitability also makes it suitable for migration testing at elevated temperatures.

Even though the accelerated conditions defined above significantly reduce the time required to determine the safety of paperboard for food packaging, it still requires 10 days to obtain a result. A number of studies have been published detailing the development of a migration test that can be completed within a working day.

Triantafyllou et al.[41] established a reliable, quick and simple method to determine potential chemical contaminants in paperboard used for food packaging. Paperboard samples were artificially contaminated with a mixture of twelve model compounds and their uptake measured into the paperboard as well as their migration into Tenax®. Migration tests were carried out at 70°C at various time intervals up to 6 hours and at 100°C at various time intervals up to 2 hours. Migration reached equilibrium after 4 hours at 70°C and after 1 hour at 100°C. In a later study[7] the migration of the model compounds into real food samples with increasing fat content was correlated with the migration values obtained with Tenax®. It was found that Tenax® is a suitable food simulant for dry foods with low and intermediate fat content such as semolina and instant baby cream. However, in the case of dry food with high fat content such as infant whole milk powder, the food shows a greater migration value than

the Tenax®. The experiments are described as a "worst case scenario" and can be used as accelerated screening for quality control purposes.

Aurela et al.[8] correlated phthalate migration into sugar at room temperature for four months (normal storage conditions) to the migration into Tenax® under accelerated conditions. It was found that the percentage phthalate migration into Tenax® at 10 days and 40°C corresponded well with the results obtained with the sugar under normal storage conditions. A shorter migration test at 2 hours and 70°C also proved to be effective. However, the migration results were found to be significantly affected by the amount of Tenax® used, the actual sample size, the addition of an internal standard (before or after exposure) and the migration vessel (gas-tight or not).

Summerfield and Cooper[42] developed a quick test for paperboard food packaging with specific focus on DBP, DiBP and DiPN. Tenax® was found to be a suitable food simulant for dry foods with a fat content of up to 25%, for paperboard used at ambient storage conditions as well as short-term contact at elevated temperatures. Furthermore, when the migration test is performed for 4 hours at 80°C, similar or greater quantities of the chemical contaminants migrated into the Tenax® as compared to food and Tenax® tested at conditions representing ambient storage.

2.7.3 Migration Modelling

Mathematical modelling is a means to predict the extent of contaminant migration from paperboard to food. In principle, for a given initial contaminant concentration present in the paperboard (which is easily measured) and taking into consideration the application parameters, the maximum migration value of the contaminant from the paperboard into the food can be calculated. This will enable rapid estimation of whether contaminant migration is within the regulatory limits.[13]

The development of predictive migration models for paperboard is difficult due to the inhomogeneous nature of the substrate. Castle[13] applied the classical diffusion models based on Fick's 2nd law, where migration is governed by the diffusion of the chemical contaminants. However, this one-dimensional model assumes that all the contaminant migrates into the food and does not account for losses due to evaporation, even though Castle overcame this problem by expressing the contaminant migration as a fraction lost from the paper. Hellén et al.[30] found that there was a threshold grammage for the validity of the one-dimensional diffusion model, where it was not applicable to paperboard of low porosity and low thickness. Poças et al.[33, 43] used a kinetic model based on the Weibull

distribution function to describe the migration of phthalates and found that the Weibull model well describes the migration of low molecular weight phthalates which presents a typical migration curve (Figure 2.8a) shape as well as the high molecular weight phthalates which present a sigmoidal migration curve (Figure 2.8b). The model is composed of two parameters. The rate parameter, τ, is determined by the diffusion coefficient and paperboard thickness and describes the rate of migration. The shape parameter, β, is determined by the initial migration rate and describes the pattern of the migration over time curve.
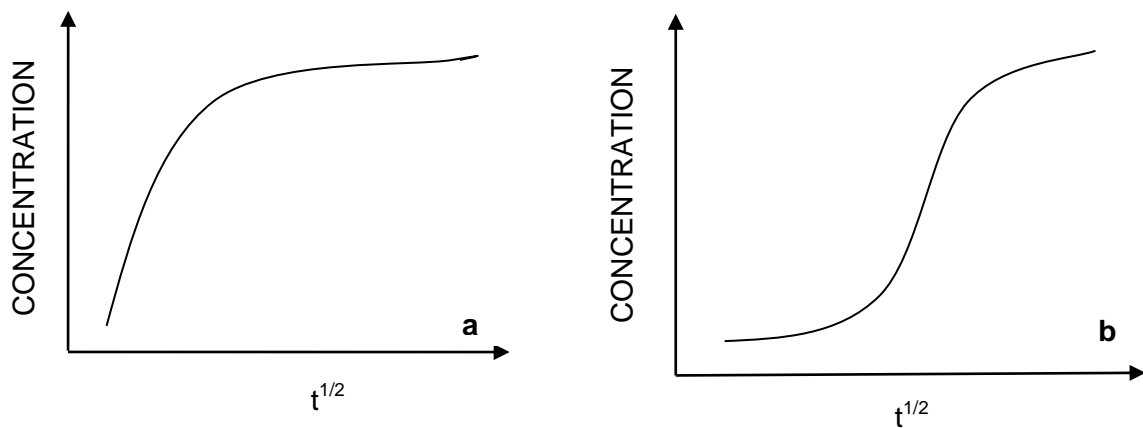
Figure 2.8:(a) Typical migration curve and (b) Sigmoidal migration curve

$$\frac{C_{(t)} - C_\infty}{C_0 - C_\infty} = 1 - \exp\left[-\left(\frac{t}{\tau}\right)^\beta\right]$$

Equation 2.11

In Equation 2.11, $C_{(t)}$ is the concentration of the chemical contaminant in the food at time, t; C_∞ is the chemical contaminant concentration in the food at equilibrium; C_0 is the initial chemical contaminant concentration in the food. When the model is applied to the chemical contaminant migration, the initial chemical contaminant concentration in the food is considered to be zero. The chemical contaminant concentration in the food, $C^f_{(t)}$, is normalised with the initial chemical contaminant concentration in the paperboard, C^P_0, to yield Equation 2.12.

$$\frac{C^f{}_{(t)}}{C^P{}_0} = \frac{C^f{}_\infty}{C^P{}_0}\left[1 - \exp\left(-\left(\frac{t}{\tau}\right)^\beta\right)\right]$$

<div align="right">*Equation 2.12*</div>

A migration experiment is used to determine $C^f{}_\infty$, *β* and τ. The migration of the chemical contaminant from the paperboard into Tenax® is monitored as the increase in chemical contaminant concentration in Tenax® over time until equilibrium is reached. This is the equilibrium chemical contaminant concentration, $C^f{}_\infty$. The shape parameter, *β,* and the rate parameter, τ, are determined by statistical analysis of the migration data using either graphical or analytical methods.[44, 45]

2.8   Functional barriers for paperboard

2.8.1   Reducing or preventing migration

A number of strategies have been proposed to minimise or reduce the migration of chemical contaminants from paperboard packaging into the food it contains. The substitution of recycled fibre as a fibre source with virgin fibre has been proposed. This is not viable in terms of cost, availability of fibre and environmental impact. Furthermore, using only virgin fibre in primary paperboard packaging does not eliminate the risk of contaminants migrating from the secondary packaging that is manufactured from recycled fibre.

Improvement in sourcing and sorting of recycled paperboard to eliminate newsprint in the case of reducing mineral oil migration has also been suggested. This is not a viable option to reduce the migration of a broad spectrum of chemical contaminants, as the chemical contaminants may originate from a wide variety of sources.

The most favourable strategy is the use of functional barriers. These can either be in the form of an inner liner bag or a barrier coating or extruded film applied directly to the paperboard. This will reduce or prevent migration of chemical contaminants from the paperboard into the food.[46, 47]

2.8.2   Evaluation of barrier properties

Fiselier and Grob[48] described the action of a barrier as a two-phase process. Initially, the chemical contaminants migrate from the bulk of the barrier-coated paperboard to the interface between the barrier film and the food or food simulant. Hence no migration from the

paperboard into the food is measured. This is referred to as the lag-time. After the lag-time, the barrier material retards the migration of the chemical contaminants into the food. A method to determine the lag-time of mineral oils for a number of different barriers was developed. This consisted of a test pack with a sheet of mineral oil-spiked copy paper, a spacer on one side of the barrier film and a polyethylene (PE) film on the other side of the barrier film to act as a food simulant. The whole assembly was encased in aluminium foil. The test packs were placed in an oven at 40°C and 60°C, and the PE film was periodically sampled. The samples were then extracted in hexane for 2 hours and the MOSH and MOAH content determined by HPLC coupled to GC-FID.[49] The method allowed the comparison of the barrier properties of various polymer films.

Ewender et al.[47] developed an automated method, based on the method of Fisilier and Grob[48], to evaluate the mineral oil permeation through barrier films such as oriented polypropylene (OPP), high density polyethylene (HDPE), polyethylene terephthalate (PET), polyamide (PA) and metalized OPP. The barrier film was placed in a specialised permeation cell, where the film separated the upper and lower space of the cell. A paperboard sample, spiked with a mixture of 15 model compounds representative of the mineral oil range of chemical structures was placed in the lower part of the cell in direct contact with the barrier film. The model compounds migrated through the barrier film into the upper part of the cell, which was constantly flushed with nitrogen. The nitrogen stream was sampled at regular intervals and migration levels determined by GC-FID. A linear correlation was found between the log of the permeation rate and the log of the partial vapour pressure of the model compounds at given temperatures. Therefore, if the vapour pressure of any mineral oil compound is known, the corresponding permeation rate can be predicted for each of the barrier films evaluated.

Song et al.[50] evaluated the chemical contaminant migration barrier properties of polypropylene (PP) film. Paperboard samples were artificially contaminated with four model compounds (anthracene, benzophenone, methyl stearate, and pentachlorophenol) simulating the types of chemical contaminants that may be found in recycled paperboard. The migration rate of these compounds was found to be inversely proportional to the thickness of the PP film. The barrier properties of the PP films were lost at high temperatures e.g. 100°C unless a sufficient thickness threshold was used in the presence of traces not exceeding 1.0 mg/kg.

Pastorelli et al.[39] developed a test method to evaluate the barrier properties of a number of plastic films used to package cake against the migration of benzophenone. The cake sample was placed in a sachet of conventional PP, as well as two multilayer films composed of polyethylene terephthalate/silicon oxide/polyethylene (PET/SiOx/PE) or

25

polypropylene/ethylene vinyl alcohol/polypropylene (PP/EVOH/PP). The cake sachets and a benzophenone spiked PE wax were placed in an air–tight container with no direct contact between them, at 70°C for 2 days and at 40°C for 10 days. Thereafter, the cake samples were disintegrated and extracted with acetonitrile for 24 hours at 70°C in an air-tight container. The extract was analysed with HPLC fitted with a diode array detector (DAD). The two multilayer films provided improved barrier properties to benzophenone as compared to the conventional PP film.

Gartner *et al.*[51] evaluated the barrier properties of coated paperboard, aluminium–coated foil and plastic foil to the migration of phthalates into infant food. The paperboard, barrier film and food material were placed in direct contact for 2 months at 40°C. Thereafter, the food material was extracted in iso-octane using an accelerated solvent extractor and the extract analysed by GC-MS. In the absence of the barrier film, the migration values of di-iso-butyl phthalate (DiBP) and di-butyl phthalate (DBP) into the food material were 6% and 5% of the initial concentration present in the paperboard, respectively. However, with the introduction of the barrier films, the migration values were reduced to below 0.1% of the initial concentration present in the paperboard.

2.8.3 The Permeation Test Method

The above studies show that it is possible to evaluate the barrier properties on a range of films. However, these methods require highly specialised and costly analytical equipment. There is a need for a simple, rapid and inexpensive method to evaluate the barrier properties of polymer films or polymer coatings toward migration of specific contaminants.

Recently, Tiggelman[16, 52] proposed an accelerated permeation method for the determination of the mineral oil barrier properties of paperboard intended for food packaging. The test method involves the exposure of one side of the paperboard sample to a saturated environment of either organic solvent vapour (n-heptane was used) or mineral oil vapour. An adsorbent material, activated carbon was placed on the opposite side in order to trap vapours that permeate through the paperboard. The adsorbent mass uptake after a predefined time period is used to calculate the vapour transmission rate per area per hour.

$$HVTR(g / m^2 / h) = \frac{W_2 - W_1}{A \times t}$$ *Equation 2.13*

where $HVTR$ (g/m^2/h) is the heptane vapour transmission rate, W_1 (grams) and W_2 (grams) are the weights of the activated carbon before and after exposure respectively, A (m^2) is the surface area of the exposed substrate and t (hours) is the exposure time.

A good correlation was reported between the mineral oil vapour transmission rate and the HVTR, which can be determined in one hour should the steady state conditions be reached. The HVTR was then correlated to the predicted shelf-life for a number of barrier films. The shelf-life is the time taken for the SML to be reached in the food or food simulant. An inversely proportional relationship was found between the log(shelf-life) and the log(HVTR) i.e. a low HVTR corresponded to a long shelf-life. This shows that the determination of the HVTR can be used to estimate a worse-case shelf-life of the barrier film. Diehl *et al.*[53] and Seyffer *et al.*[54] used a similar method of mass transfer to test the mineral oil barrier properties of coatings developed for paperboard applications. However, the mineral oil simulant, hexane, was placed inside a similar sample cell and the permeability of the film measured gravimetrically as a function of cell weight loss. The HVTR value was compared to the mineral oil breakthrough time determined using the same method described by Fiselier and Grob.[48] Results showed an inversely proportional relationship between the HVTR value and the mineral oil breakthrough time i.e. a low HVTR value corresponded to a long mineral oil breakthrough time. A quick check method was developed to evaluate the barrier properties of barrier coatings to the migration of mineral oils.

CHAPTER 3

EXPERIMENTAL

3.1   General practices

The laboratory was regulated by an air-conditioning system at 23°C, and referred to as room temperature throughout the study.

Gloves were worn at all times to prevent contamination of the samples.

Glassware and extraction cells were washed, dried at 160°C for 2 h and allowed to cool to room temperature before use. Immediately before use, glassware was rinsed with HPLC grade acetone.

Tenax® was washed with HPLC grade acetone as described in Section 3.5, dried in an oven at 160°C for 6 h and allowed to cool to room temperature before use. The Tenax® was stored in a clean, dry air-tight glass container, with aluminium foil placed over the opening of the container.

Only HPLC grade solvents were used. The highest purity of the standards and internal standards available from suppliers were used. All carrier gases used (helium for the GC-MS, nitrogen for the ASE350) were baseline 5.0 grade.

Spiked paperboard samples were used immediately after preparation. A spiked, uncoated paperboard sample was included with each migration experiment. The concentration of DiBP, DBP and DEHP present in the uncoated paperboard sample was determined and used to calculate the percentage migration of DiBP, DBP and DEHP from the various coated paperboard samples into Tenax®. As such, all migration results were reported as a percentage of the original amount of the compound present in the paperboard after spiking. The results reported in this study were based on the average of two replicates.

3.2   Sample preparation

3.2.1   Calibration standards

Di-n-butyl phthalate (DBP), di-iso-butyl phthalate (DiBP) and bis(2-ethylhexyl) phthalate (DEHP) with a purity of 99% were supplied by Sigma Aldrich. The calibration standards were made up in HPLC grade acetone. The internal standard, di-butyl phthalate-3,4,5,6-d_4 (d-DBP) with a purity of 98% was supplied by Sigma Aldrich. The calibration standards were

prepared in 10 mL volumetric flasks with the concentration being varied from 2.0-1250 µg in 10 mL. The calibration curve was constructed by plotting the response ratio of the analyte peak to the internal standard peak against the mass of analyte in the 10 mL volumetric flask. The internal standard was prepared as a 100 ppm solution in acetone. 25 µL of the internal standard was added to each of the calibration standards as well as the unknown samples.

3.2.2   Barrier coated paperboard

A custom-built K Control Coater (Scientific Manufacturing CC., South Africa) was used to apply the barrier coatings to the paperboard substrate. The thickness of the applied film was varied using standard K101 close-wound metering bars (No. 1, 2, 3 and 7) and a smooth metering rod.

3.2.2.1   General preparation

Seven different barrier coatings were used, and applied to the paperboard as one-layer and two-layer coating configurations. The barrier coatings were applied to the back liner of a 350 g/m^2 paperboard substrate manufactured from recycled fibre. The paperboard was fixed onto a flat surface and the coating pooled close to the top of the paperboard. A metering rod was applied to the coating pool and drawn down the length of the paperboard, thereby metering a precise coating thickness on the paperboard. The wet coating thickness was controlled by the cross-sectional area of the grooves between the wire coils of the rod.[55] A schematic of the wire-wound rod is shown in Figure 3.1. The thickness of the barrier coating applied to the paperboard was increased in order to produce samples of varying barrier efficiency. This was achieved by applying single- and double-layer coatings to the paperboard, using coating rods with wire windings of increasing diameter around the coating rod.[56]
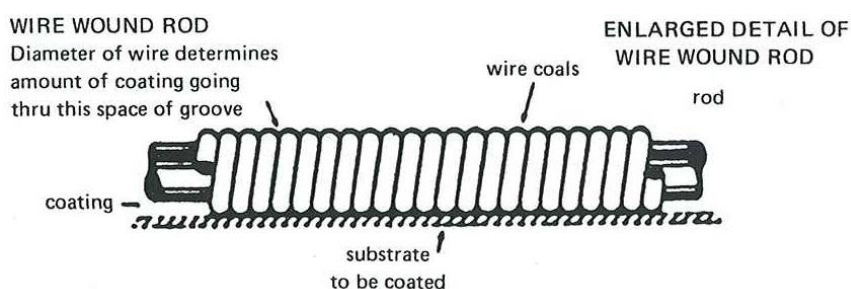
Figure 3.1: Wire-wound rod design.[55]

3.2.2.2 Varied pinhole density

The PVDC barrier polymer was subjected to a shear rate of 1300 rpm for 0, 1, 5, 7, and 10 minutes to incorporate air into the barrier polymer. The coating was applied to the paperboard surface as a single-layer configuration using the No. 7 coating rod and allowed to dry. Upon drying, pinholes formed upon rupture of the air bubbles.

3.2.3 *Sample spiking with model contaminants*

The principle of the spiking method used by Poças *et al.*[33] was employed. The spiking solution was composed of an equal volume of DBP (2500 ppm), DiBP (2500 ppm) and DEHP (2500 ppm). During the course of the study amendments to the experimental design in terms of the spiking equilibration time, the spiking volume, the sample area and the migration testing time were required and are described below.

3.2.3.1 Spiking equilibration time

The spiked samples were allowed to equilibrate at 23°C for 48 h and at 60°C for 24 h. The latter conditions resulted in higher spiking concentrations in the paperboard samples and were used throughout the study.

3.2.3.2 Sample area

A sample area 0.6 dm^2 (diameter of 88 mm) was used for Migracell$^®$ migration cells. A blotting paper disc with an area of 0.6 dm^2 was placed on a clean, dry watch glass and 4 mL of the spiking solution was applied to the blotting paper surface and left to air-dry for 25 minutes. To spike the paperboard sample with an area of 0.6 dm^2, the spiked blotting paper disc was placed in contact with the non-barrier side of the paperboard, wrapped in aluminium foil (100 mm wide and 300 mm long) and stored at 60°C for 24 h. Thereafter, the blotting paper was removed and the paperboard sample used for the migration analysis. A sample area of 0.2 dm^2 (52 mm diameter) was used for the immersion cell (A) as shown in Figure 3.3. The volume of the spiking solution applied to the 0.2 dm^2 blotting paper disc was reduced to 1.3 mL. The concentration of the model compounds present in the blotting paper as well as in the paperboard after contact with the blotting paper was confirmed by direct extraction in acetone and analysis of the extract by GC-MS (See Section 3.6).

3.2.3.3 Migration testing time

The blotting paper was removed from the paperboard sample after the predetermined equilibration time when the migration test was performed at 60°C for 24 h and 3 days. When the migration tests were performed for 28 days at 23°C, the spiked blotting paper was left in contact with the paperboard sample for the duration of the migration test.[47, 48]

3.2.3.4 Spiking volume

The spiking volume was reduced to validate the proposed correlation. The spiking volume was reduced by a half and a quarter of the original spiking volume by diluting the original spiking solution with HPLC grade acetone. The same volume of the spiking solution was used to prepare the half- and quarter-spike samples as the original spiked samples. Table 6.1 shows the volumes of the original spike solution and HPLC grade acetone required to prepare the half- and quarter-spike solutions.

Table 3.1: *Preparation of the spike solutions for validation.*

Spike solution	Original spike solution (mL)	Acetone (mL)
1.00	4	0
0.50	4	4
0.25	4	12

3.3 Permeation tests

3.3.1 Heptane vapour transmission rate (HVTR)

The base of an aluminium permeation cell containing 4-7 g activated carbon was weighed and the mass noted, W_1. The coated paperboard substrate was placed into the lid of the cell and fastened to the base of the cell with the coated side of the substrate facing outward. The cell was placed in a desiccator saturated with heptane vapour (23°C) for the defined exposure time. After the exposure time had elapsed, the cell was removed from the

desiccator. The lid of the aluminium cell was removed and the base of the cell weighed, W_2. The mass uptake of the activated carbon due to exposure to the saturated heptane environment was used to calculate the HVTR using Equation 3.1. The standard exposure time is 1 h; however, exposure times of 3 h, 7 h and 24 h were also used. The HVTR result after the exposure time were normalised to 1 h.

$$HVTR(g/m^2/h) = \frac{W_2(g) - W_1(g)}{Area(m^2) \times time(h)}$$

Equation 3.1[52]

3.4 Migration tests

3.4.1 Exposure conditions

Once the migration cells had been assembled as described in 3.4.2 and 3.4.3, two different exposure conditions were used. Initially, the cells were exposed for 24 hours at 60°C before extraction of the Tenax®. The migration test was later also performed at 23°C for 28 days and at 60°C for 3 days.

3.4.2 One-sided migration cell

A MC-60 Migracell® migration cell (Fabes Forchungs GmbH) with an exposure area of 0.5 dm² was used (See Figure 3.2). The white seal and the aluminium plate were placed onto the base of the cell. The spiked paperboard sample was placed on the aluminium disc, with the barrier coated side facing upward. The red seal and the cell lid were placed on top of the sample. The cell was sealed using a springform clamp. The screw-top lid was removed from the top of the cell and two heaped spoonfuls (± 1.5 g) of Tenax® poured into the cell using a funnel. The funnel was then removed and the screw-top lid refitted. The cell was gently shaken to evenly distribute the Tenax® over the sample surface. The cell was then exposed to the predefined migration test conditions.
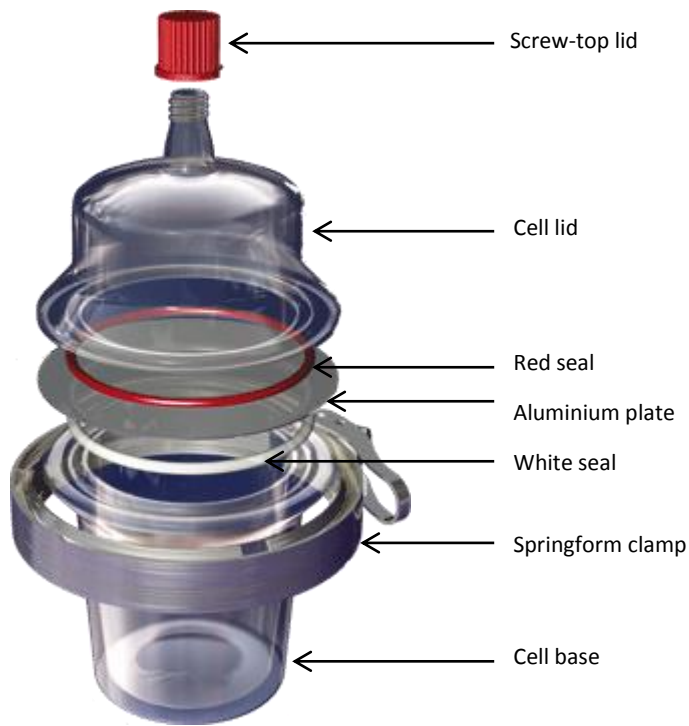
Figure 3.2: *Migracell® used for one-sided migration testing.[57]*

3.4.3 Immersion cell

Due to limited supply of the Migracell® migration cells, an alternative setup had to be utilised. A weighing bottle with a fitted lid, having a diameter of 55 mm and a depth of 30 mm was used as an immersion cell. A strip of foil (65 mm wide and 200 mm long) was cut and the paperboard sample (diameter of 52 mm) was placed onto the foil, with the barrier coated side facing downwards as shown in Figure 3.3. The dried, spiked blotting paper (diameter of 52 mm) was placed on top of the paperboard sample (B) and enclosed by the foil (C). After the equilibration period, the foil sandwich was opened and the blotting paper removed. The foil sandwich was resealed and placed onto a flat surface, with the barrier coated side facing upwards. A die (diameter of 50 mm) and scalpel were used to expose the barrier coated side of the paperboard (D). The sample was placed into the immersion cell, with the exposed barrier coated surface facing upwards and a heaped spoonful (± 0.75 g) of Tenax® evenly distributed across the sample surface (E). The immersion cell was sealed with its glass lid and exposed to the predefined migration test conditions (F).
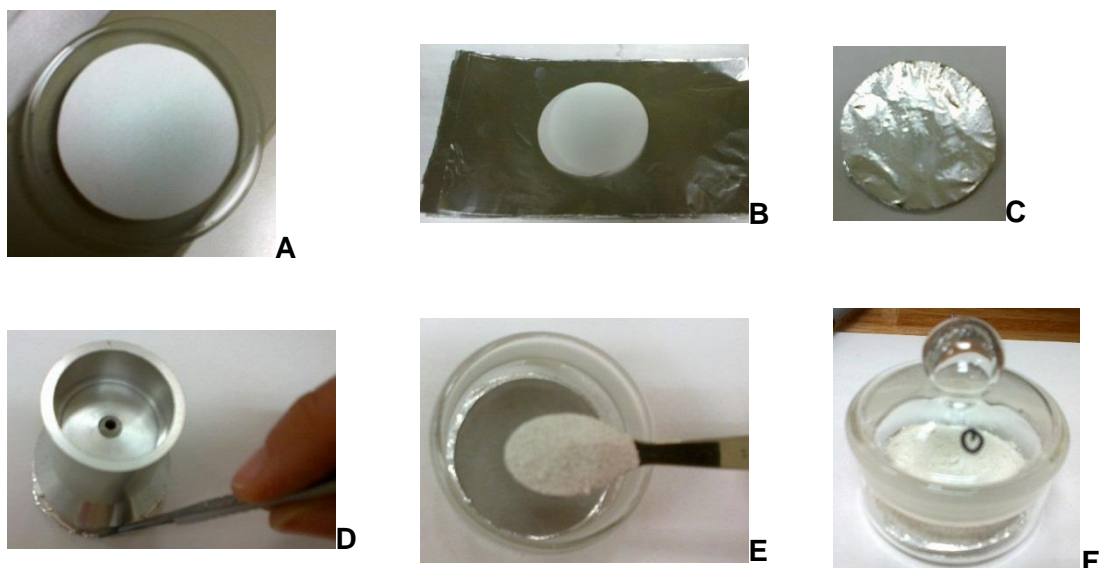
Figure 3.3: *Preparation for migration test using the immersion cell. See Section 3.4.3 above for the description of the preparation steps.*

3.5 Extraction conditions

Extractions were performed using a Dionex Accelerated Solvent Extractor ASE350. The ASE350 was equipped with a solvent controller and operated at 60% rinse volume and 100 s purge. The extractions were carried out in 22 mL ASE extraction cells using acetone at 40°C. A heating time of 5 min and a static time of 10 min were used, with two cycles for each cell.

3.5.1 Paperboard

The paperboard was cut into small pieces approximately 1 cm x 1 cm in size. A 22 mL ASE extraction cell, with a cellulose filter fitted in the base, was filled with approximately 5 g of the paperboard sample and spiked with 25 µL of a 100 ppm d-DBP internal standard solution.

3.5.2 Tenax

After the migration test period elapsed, the Tenax was decanted into a 22 mL ASE extraction cell, with a cellulose filter fitted in the base and spiked with 25 µL of a 100 ppm d-DBP internal standard solution.

3.5.3 Recovery analysis

The efficiency of the extraction method was evaluated by comparing the concentration of a known solution, such as one of the calibration standards, to the concentration of the same known solution that was exposed to the extraction conditions. The recovery was expressed as a percentage

$$\% \, RECOVERY = \frac{Concentration_{EXTRACTED}}{Concentration_{STANDARD}} \times 100$$ *Equation 3.2*

A heaped spoonful (± 0.75 g) of Tenax was placed into a 22 mL ASE extraction cell, with a cellulose filter fitted in the base. 250 µL of one of the calibration standards was added to the ASE cell.

3.6 Extract Concentration

A Biotage TurboVap LV Concentration Evaporator Workstation was used. The sample extracts obtained from the Dionex ASE350 were concentrated under a constant stream of nitrogen at 40°C until approximately 1 mL of the extract remained in the ASE vial. The concentrated extract was decanted into a 1.5 mL vial, to fill approximately one third of the volume of the vial. The vial was then filled with acetone and closed with the screw-cap lid.

3.7 GC-MS Analysis

Samples were analysed with a Thermo Scientific Trace Ultra gas chromatograph fitted with a Thermo Scientific ISQ Mass selective (MS) detector. A 5% phenyl, 95% polysiloxane capillary column with a length of 30 m and an internal diameter of 0.25 mm was used. The column temperature program started at 40°C for 2 min. The temperature was ramped at 15°C/min to 280°C and held constant for 15 min. Thereafter, the temperature was reduced to 200°C for 10 min as a post run conditioning. Helium was used as the carrier gas at a flow rate of 1.2 mL/min in constant flow mode with the vacuum compensation on. The injector port was maintained at 220°C and an injection volume of 1 µL in splitless mode. The ISQ-MS was operated in electron impact (EI) ionisation mode, scanning from 35-650 amu with dwell time of 200 ms. Time-scheduled selected ion monitoring mode (SIM) was used for quantification,

using m/z 149 for the native phthalates and m/z 153 for the deuterated phthalate. The MS transfer line temperature was maintained at 280°C and the ion source at 200°C.

3.7.1 Limit of detection

The limit of detection was determined as the lowest concentration where the signal to noise ratio (*S/N*) was greater or equal to three. The calibration standard with the lowest concentration was diluted and injected into the GC-MS. The intensity of the signal peak i.e. DiBP, DBP and DEHP was determined and compared to the intensity of the baseline noise. If the *S/N > 3*, the calibration standard was further diluted and the injection repeated until the *S/N ≤ 3.*

3.7.2 Limit of quantification

The limit of quantification was set at ten times the LOD.

3.8 Dynamic Scanning Calorimetry Analysis (DSC)

The Tg and thermal properties of the barrier coatings were determined using a Q100 differential scanning calorimeter from TA instruments fitted with a refrigerated cooling system cooling unit. The instrument was operated in the temperature range from -50°C and 250°C at a rate of 10°C/min in a nitrogen atmosphere.

3.9 Surface defect test

Methanol was applied to the surface of coated paperboard (10 cm x 10 cm) and inspected visually for defects. Surface defects such as cracks and pinholes will appear as darkened areas on the surface.

3.10 Pinhole density

An image of the coated paperboard substrate was captured during the surface defect test. A grid comprised of 100 blocks was applied to the surface defect test image. The number of blocks in the grid occupied by a pinhole(s) were counted and expressed as a percentage.

3.11 Statistical analysis

3.11.1 Student's t test

The Student's t test was applied to the part of this study where the pinhole density was varied whilst the coating weight was kept constant. The null hypothesis for the Student's t test was set that the average coating weight for each individual shear interval was not significantly different from the average coating weight of all the shear intervals. A confidence level of 95% was used.

CHAPTER 4

EFFICIENCY OF SPIKING METHOD

4.1   Introduction

A number of methods have been used to spike paperboard samples with a known quantity of model chemical contaminants. The most common method is immersion of the paperboard samples in a solution of known model chemical contaminants for a predetermined time period. Thereafter, the samples are allowed to dry and wrapped in aluminium foil until use.[7, 47, 48, 50] Handmade paperboard sheets have also been prepared by incorporating known quantities of model chemical contaminants into a pulp slurry before forming the sheet.[10] However, these are not suitable options for paperboard samples with a functional barrier applied to one side of the sheet. Aurela *et al.*[58] used a direct method of spiking paper plate samples with a barrier layer by applying several spots of the model compound solution onto one side of the sample. Poças *et al.*[33] on the other hand spiked paper samples indirectly via contact with a sheet of blotting paper that was spiked by immersion. The paperboard sample to be tested was placed in a sandwich of blotting paper, wrapped in aluminium foil and left for two days at room temperature to equilibrate.

4.2   Limit of detection (LOD)

The LOD for DiBP, DBP and DEHP was found to be less than 0.2 µg in 10 mL for all three phthalates.

4.3   Limit of quantification (LOQ)

The LOQ for DiBP, DBP and DEHP was 2 µg in 10 mL for all three phthalates.

4.4   Recovery

The recovery is an indication of the efficiency of the extraction method and was determined as described in Chapter 3. The recoveries for DiBP, DBP and DEHP were determined to be 95%, 91% and 88%, respectively.

4.5 The spiking method

The principle of the spiking method used by Poças *et al.*[33] was employed in this study, but spiked blotting paper was placed only on the non-barrier side of the paperboard. The spiking solution contained amounts of the model chemical contaminants that theoretically lead to a concentration in the blotting paper of 4.2 mg/dm^2 for each chemical contaminant, should no loss due to evaporation occur during the drying phase of the blotting paper spiking procedure (as described in Chapter 3). However, the actual concentrations of the chemical contaminants in the blotting paper were measured to be 0.40 mg/dm^2 for DiBP, 0.40 mg/dm^2 for DBP and 0.61 mg/dm^2 for DEHP after the drying process. This is related to the vapour pressure. DiBP has the greatest vapour pressure and as such will partition into the gas phase at a faster rate than DBP and DEHP. Thus, more DiBP will be lost due to evaporation than the lower vapour pressure compounds.

Table 4.1: *Vapour pressure of model contaminants.*[59]

Model contaminant	Vapour pressure @ 20-25ºC (kPa)
DiBP	1.0×10^{-5}
DBP	9.7×10^{-6}
DEHP	1.3×10^{-8}

Once the concentrations of the chemical contaminants present in the blotting paper were known, the quantity of the chemical contaminants that migrated from the blotting paper into the paperboard during the equilibration time had to be determined. This was done by two separate extractions in acetone of the spiked blotting paper and the paperboard after an equilibration time of 48 h, followed by quantification by GC-MS. The concentration in mg/dm^2 of the model compounds transferred from the blotting paper to the paperboard is shown in Figure and Table 4.2. The concentration of the chemical contaminants present in the paperboard was also expressed as percentage transfer from the blotting paper into the paperboard as shown in Figure 4.2. DiBP and DBP both showed approximately 50-55% transfer and DEHP only showed about 10% transfer. This is again related to the vapour pressure as described above. However, in this case, the blotting paper and paperboard were

in a confined system, where the model compounds can no longer escape to air via the gas-phase, but could only partition between the blotting paper and the paperboard.
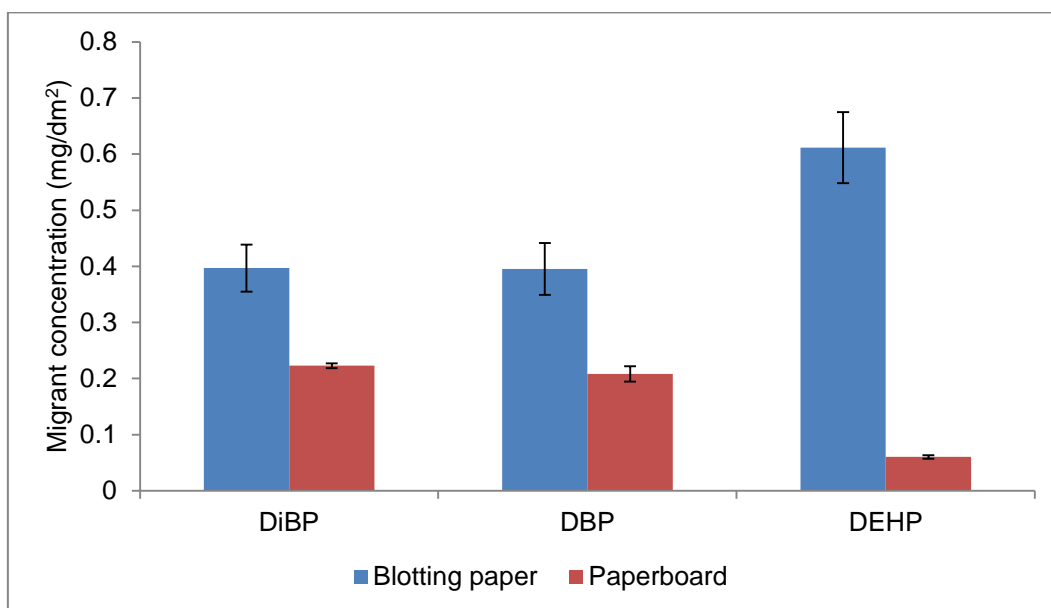
Figure 4.1: *Concentration of the model compounds transferred from the blotting paper to the paperboard with equilibration at 23°C for 48 h.*

Table 4.2: *Concentration of the model compounds present in the blotting paper and the spiked paperboard after equilibration at 23°C for 48 h.*

Substrate	Migrant concentration (mg/dm^2)		
	DiBP	**DBP**	**DEHP**
Blotting paper	0.40 ± 11%	0.40 ± 12%	0.61 ± 10%
Paperboard after spiking	0.22 ± 2%	0.21 ± 7%	0.06 ± 5%

4.6   The effect of equilibration conditions

Since the amount of DEHP transferred from the blotting paper to the paperboard was found to be very low, methods to enhance the transfer efficiency were considered. Two strategies could be used, namely to increase the concentration of the DEHP in the spiking solution or to

increase the temperature of the equilibration period. A temperature increase was attempted to increase the vapour pressure[60] of DEHP, hence expecting faster partitioning into the gas phase. The equilibration conditions were thus changed to 24 hours at 60ºC. The percentage transfers of the model chemical contaminants for the two equilibration conditions are shown in Figure 4.2 and Table 4.3. The accelerated conditions showed faster and increased transfer of DiBP, DBP and DEHP from the blotting paper to the paperboard.
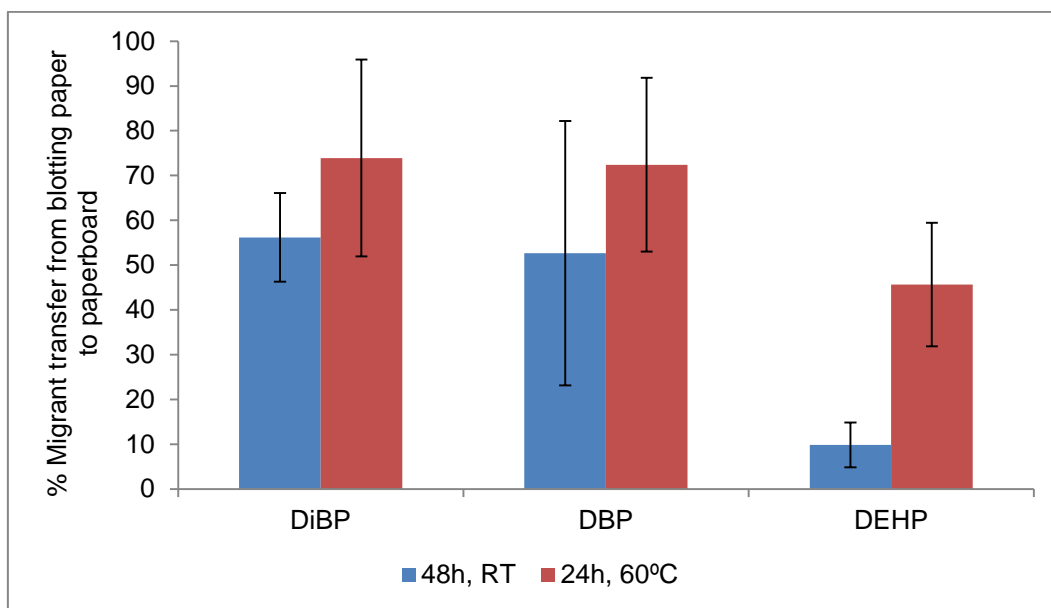
Figure 4.2: *Comparison of percentage contaminant transfer from the blotting paper to the uncoated paperboard at different equilibration conditions.*

Table 4.3: *Comparison of percentage contaminant transfer from the blotting paper to the uncoated paperboard at different equilibration conditions.*

Equilibration conditions	Migrant transfer from blotting paper to paperboard (%)		
	DiBP	DBP	DEHP
48 h, 23°C	56	53	10
24 h, 60°C	74	72	46

The reproducibility of the spiking method was monitored throughout the course of the study. The reproducibility was found to be poor in light of the relative standard deviation ranging from 30% to 35% for the three phthalates. This could be related to the inhomogeneity of the blotting paper and the paperboard. It could also be due to different rates of evaporation during preparation of the blotting paper owing to slight differences in temperature from day to day. As such, the results of the migration tests that will be discussed in the remainder of this study will be expressed as a percentage of the contaminant that was originally present in the paperboard after spiking.

4.7   Conclusion

A method to spike the paperboard samples with known quantities of DiBP, DBP and DEHP was established. The reproducibility of the method was poor, with relative standard deviations of up to 35% observed for all three phthalates. This necessitated that the migration of DiBP, DBP and DEHP into Tenax[®] be expressed as a percentage of DiBP, DBP and DEHP present in the paperboard.

CHAPTER 5

CORRELATION BETWEEN HVTR AND SPECIFIC MIGRATION FOR DIFFERENT BARRIER POLYMERS

5.1 Introduction

A number of studies have been published regarding the development of migration test methods for barrier coated paperboard. Pastorelli *et al.*[39] compared the barrier properties of PP, PP/EVOH/PP and PET/SiOx/PE films used as the primary barrier for cakes packaged in paperboard containers. The migration of benzophenone from the printed paperboard into the cakes through these three barrier films using two migration conditions, 40°C for 10 days and at 70°C for 2 days were compared. Similar migration trends were observed. Song *et al.*[50] evaluated the barrier property of PP films for paperboard packaging used in high-temperature applications such as microwaveable or ovenable packaging. The migration of anthracene, benzophenone, methyl stearate and pentachlorophenol through the PP film was tested at 100°C for 2 h. It was found that PP was not an effective barrier for paperboard packaging upon use at 100°C for extended periods. Choi *et al.*[61] evaluated the barrier property of PE coated paperboard to anthracene, benzophenone, dimethyl phthalate, methyl stearate and pentachlorophenol, at 10°C and 24°C for 21 days. The relative rate and the degree of migration for benzophenone and dimethyl phthalate varied depending on the temperatures.

It has been well documented that the nature of the barrier polymer has an effect on the migration of specific penetrant molecules.[19, 21, 62, 63] It is governed by properties such as polarity, cohesive energy (i.e. chain stiffness), degree of chain packing, crystallinity, inertness to the permeating molecule, the Tg and the presence of fillers or plasticisers.

5.2 The proposed correlation between HVTR and specific migration

In this work, seven different barrier polymers were used. These polymers were several styrene acrylic, a styrene butadiene, a polyvinylidene chloride (PVDC) and a polymer containing an inorganic pigment. It should be noted that the barrier polymers used were commercially available products. The basic chemical structure was known as shown in Table 5.1 and Figure 5.1. However, other properties such as the addition of fillers or other additives and the degree of crystallinity were not disclosed by the supplier. These properties may also influence the barrier properties of the polymer.

Table 5.1: *Description of the barrier polymers used and glass transition temperatures.*

Barrier label	Polymer type	Tg (°C)
Barrier A	Styrene-Acrylic polymer	13.4
Barrier B	Polymer containing inorganic pigment	3.5
Barrier C	Styrene-Acrylic polymer	-2.8
Barrier D	Carboxylated Acrylate co-polymer	50.8
Barrier E	Styrene Acrylic	12.1
Barrier F	Anionic Carboxylated Styrene Butadiene	7.2
Barrier G	Polyvinylidene Chloride (PVDC)	16.6

Styrene-Acrylic   Styrene-butadiene   PVDC
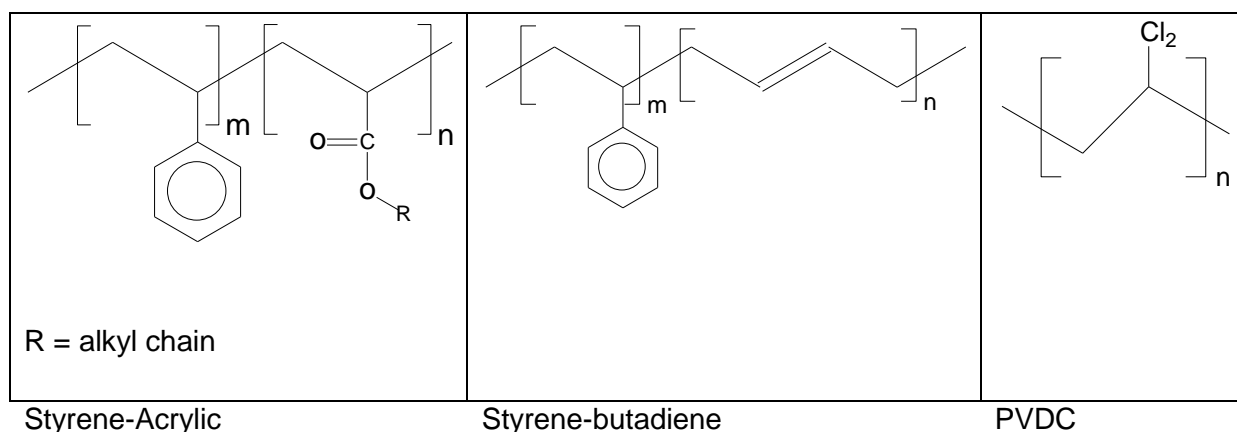
Figure 5.1: *Basic chemical structures of the barrier polymers used.*

The seven barrier polymers were applied to the paperboard substrate as double-layer barrier coating configurations to ensure complete coverage of the paperboard surface. An eighth configuration using Barrier B as the first layer and Barrier D as the second layer was also included. This was done because the double-layer configuration of Barrier D showed poor surface coverage and Barrier B is commonly used as the first layer in double layer coating configurations. An uncoated configuration was also included as a reference. The HVTR

(23°C for 1 h) and the specific migration (60°C for 24 h) of DiBP and DBP for each configuration was determined and plotted against each other (as shown in Figure 5.2) to determine whether a correlation exists between the HVTR and specific migration. The behaviour of DEHP was excluded as the migration levels measured were below the limit of quantification of 2 µg in 10 mL. It should be noted that the migration of DEHP observed in Chapter 4 was for uncoated paperboard samples. However, in this case, the application of the barrier coating configurations appeared to impede the migration of the DEHP from the paperboard into the Tenax®. Table 5.2 details the barrier polymers used for the different configurations as well as the HVTR and specific migration for each configuration. The coating configurations (referred to as CONFIG in the remainder of the text) were arranged in order of increasing HVTR.

Table 5.2: *The HVTR and specific migration (24 h at 60°C) of the eight barrier polymer configurations and the uncoated configuration used.*

	Configuration number								
	1	**2**	**3**	**4**	**5**	**6**	**7**	**8**	**9**
First Layer	Barrier G	Barrier B	Barrier E	Barrier B	Barrier F	Barrier C	Barrier A	Barrier D	None
Second Layer	Barrier G	Barrier D	Barrier E	Barrier B	Barrier F	Barrier C	Barrier A	Barrier D	None
HVTR (g/m^2/h)	4.0	6.0	8.6	10.2	12.6	14.6	24.6	50.5	136.4
DiBP Migration (%)	6.2	2.0	43.6	40.5	51.4	52.9	68.9	26.8	87.9
DBP Migration (%)	3.7	2.9	29.9	28.6	33.9	36.9	63.6	16.4	71.7

Figure 5.2(a) shows the correlation between the HVTR and the specific migration of DiBP and DBP. Figure 5.2(b) shows a magnified view of the first eight points. An initial rapid increase in the specific migration of DiBP and DBP is seen up to a HVTR of 25 g/m^2/h. This is followed by a more gradual increase in the specific migration of DiBP and

DBP for the HVTR above 25 g/m^2/h. A poor correlation between the HVTR and the specific migration of DiBP and DBP was observed, both only showing a correlation coefficient of $R^2 = 0.4$.[64]
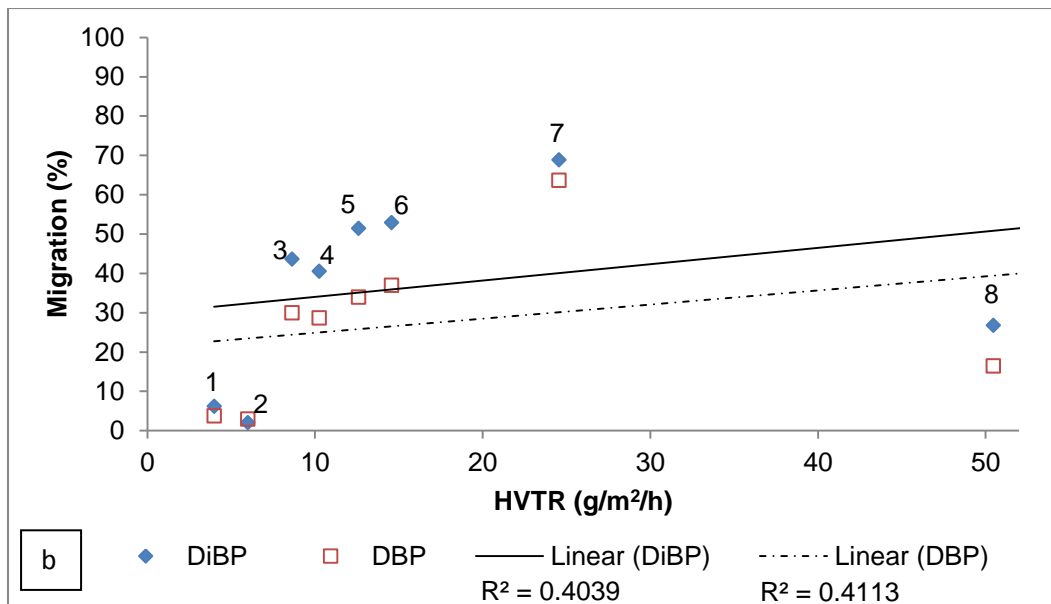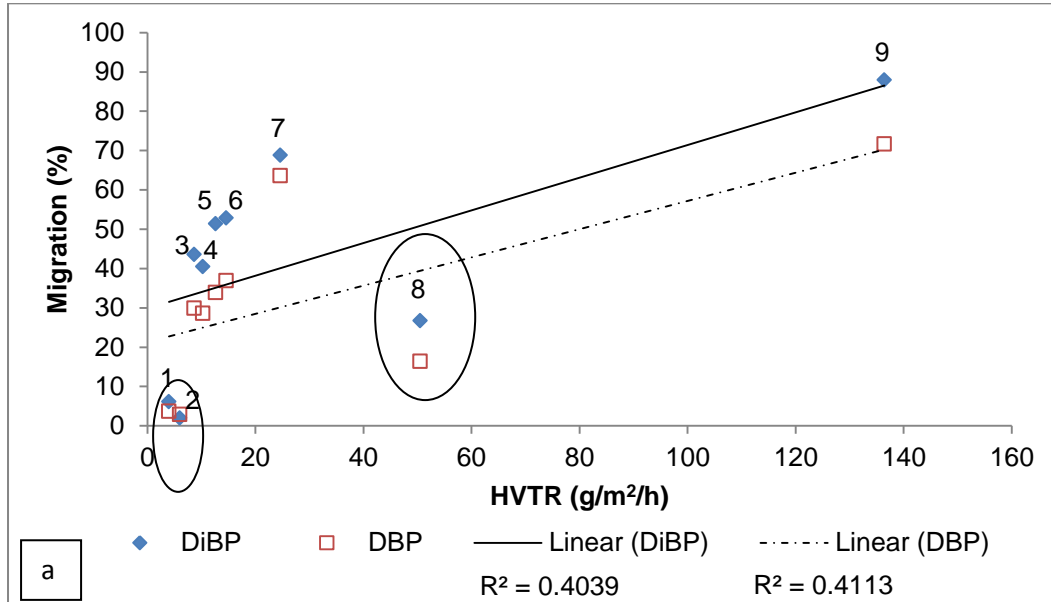
Figure 5.2: (a) Correlation between the specific migration of DiBP and DBP at 60°C and HVTR at 23°C for the barrier polymer configurations. (b) Magnified view of the first eight points.

A general trend was observed that the specific migration increased as the HVTR increased. However, two points deviated from this trend, namely Config 2 and Config 8 (the two points circled in Figure 5.2). These configurations both contain Barrier D as the second layer of the coating configuration. The properties of Barrier D were examined (Table 5.1) and the Tg of the barrier polymer was found to be 50°C. The Tg of the other six barrier polymers are all below 23°C.

Table 5.3 shows the relationship between the HVTR, migration testing temperature and the Tg of the barrier polymers. The HVTR test is performed at 23°C and the specific migration test is performed at 60°C. In the case of Barrier D, the barrier polymer is in the glassy state (T < Tg) during the HVTR test and in the rubbery state (T > Tg) during the migration test. The mechanism of diffusion of chemical contaminants differs significantly for polymers in the rubbery and glassy states.[25, 65] A better understanding of how the migration mechanisms are influenced above and below the Tg is necessary to comprehend the deviation observed above. This will clarify the validity of correlating the HVTR and the specific migration in the case of the configuration containing Barrier D, which will be further evaluated in the following section.

Config 2 was the only configuration that was made up of two different barrier polymers. If Barrier D had been replaced by any of the other barrier polymers as the top layer, it is unlikely that it would have deviated from the observed trend. This is related to the Tg of the barrier polymers. The Tg of the remaining barrier polymers are below 23°C and as such the polymers would be in the same state for both the HVTR and the migration test as shown in Table 5.3. This is however speculative as no data is available to substantiate the claim.

Table 5.3: Relationship between HVTR testing temperature, migration testing temperature and the Tg of the barrier polymers.

Configurations	HVTR at 23 °C	Migration at 60 °C
2, 8	T < Tg	T > Tg
1, 3, 4, 5, 6, 7, 9	T > Tg	T > Tg

5.3 Effect of glass transition temperature on the correlation between HVTR and specific migration

The transport behaviour of a penetrant though a barrier film is quite different above and below the glass transition temperature. The difference in the transport behaviour can be described by the effect of pressure or concentration and temperature on the permeability, diffusion and solubility coefficients.[65]

Above the glass transition temperature, the polymer is in the rubbery state and transport is considered to occur by a single-mode mechanism. As mentioned in Chapter 2 (2.4.3), penetrant transport occurs as a series of jumps between free-volume holes that are redistributed through the polymer due to the continual movement of the polymer chains. The diffusion coefficient is directly proportional to the temperature and an increase in the temperature will increase the mobility of the polymer chains, thereby accelerating the redistribution of the free-volume. A change in pressure may result in two opposite effects on the diffusion coefficient. An increase in pressure will lead to compaction of the polymer, reducing the available free volume and thus reducing the diffusion coefficient. However, should the penetrant molecules plasticise the compacted polymer this will increase the mobility of the polymer chains, allowing redistribution of the free volume and thus increasing the diffusion coefficient. The solubility of a penetrant in the polymer film is determined by the amount of vacant free volume. It is directly proportional to pressure as defined by Henry's law. The solubility coefficient is inversely proportional to temperature in the case of condensable organic vapours.[20, 21, 65, 66]

Below the glass transition temperature, the polymer is in the glassy state and transport is considered to occur by a dual-mode mechanism. Two distinct free-volume domains occur within the glassy polymer, namely trapped free-volume and mobile free-volume. As mentioned in Chapter 2 (2.4.3), the trapped free-volume is not active in the diffusion process. The diffusion coefficient is dependent on the ability of the mobile free-volume to be redistributed under the influence of temperature and pressure. The adsorption of the penetrant into the glassy polymer will occur by different mechanisms in the two free-volume domains. In the case of the mobile free-volume, adsorption follows Henry's law, where the amount of vacant free-volume determines solubility. In the case of the trapped free-volume, a Langmuir type adsorption applies, where the interaction between the polymer and the penetrant determines solubility.[20, 21, 65, 66]

Table 5.4: *Transport behaviour of organic gases and vapours in polymer films.*[21]

Temperature in relation to Tg	Diffusion model
T > Tg Rubbery polymers	Single-mode diffusion
T < Tg Glassy polymers	Dual-mode sorption

The migration tests for the eight barrier coating configurations and the uncoated paperboard sample evaluated in this work were repeated at 23°C for 28 days. In these conditions, Barrier D is in the glassy state during both the HVTR and the migration test. The remaining barrier polymer configurations were included for comparative purposes. The correlation between HVTR determined at 23°C for 1 hour and the specific migration of DiBP and DBP determined at 23°C for 28 days is shown in Figure 5.3a and Table 5.5; a magnified view of the first eight points is shown in Figure 5.3b.

Config 2 and Config 8 previously deviated from the trend observed in Figure 5.2 when the migration test was performed at 60°C. When the migration test is performed at 23°C, Config 2 and Config 8 now follow the observed trend. The correlation between the HVTR and the specific migration is improved, but still poor, showing a correlation of $R^2 = 0.7$ for DiBP and $R^2 = 0.6$ for DBP. The barrier polymer is in the glassy state for both the HVTR and the migration test. Therefore the transport of the heptane vapours used in the HVTR test and the DiBP and DBP in the migration test will take place via the same diffusion mechanism. This illustrates that the Tg of the barrier polymer should be taken into consideration before attempting to correlate the HVTR performed at 23°C and the migration performed at 60°C as migration occurs by different mechanisms in the glassy and rubbery states.[19, 21] In addition to the Tg of the polymer, the testing time and temperature should also be taken into consideration since the HVTR is determined at 23°C for 1 h and the specific migration at 60°C and 23°C for 24 h and 28 days, respectively.
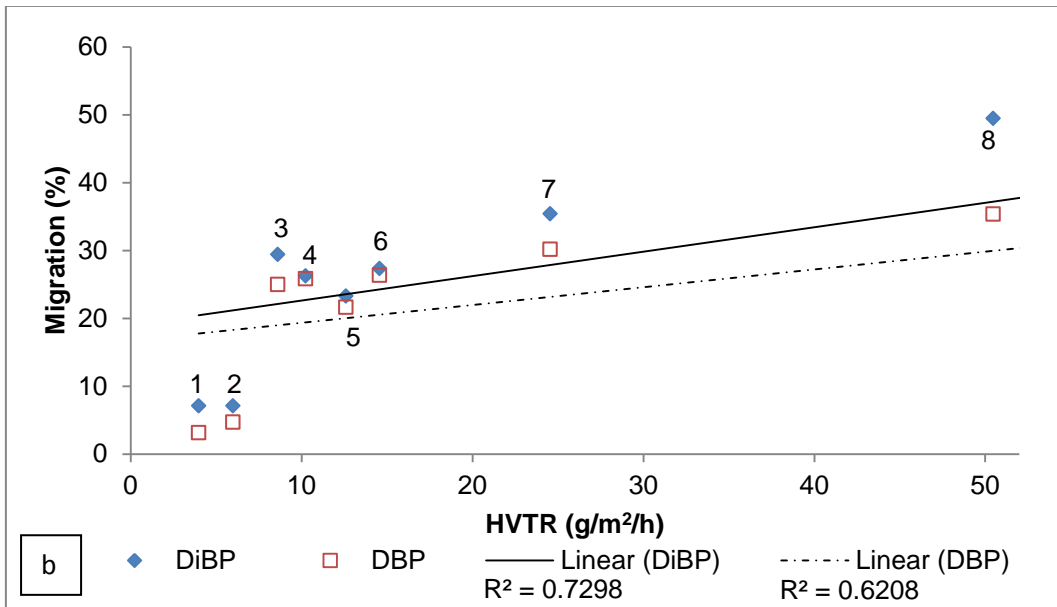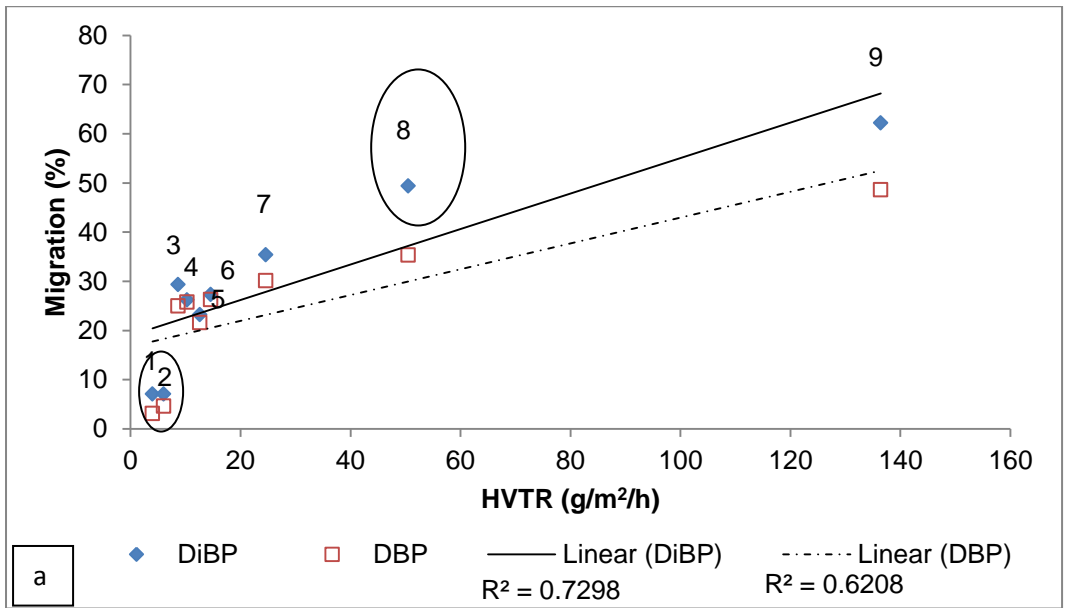
Figure 5.3: (a) Correlation between the specific migration of DiBP and DBP at 23°C and HVTR as a function of different barrier coatings. (b) Magnification of the first eight points.

Table 5.5: *The HVTR and specific migration (28 days at 23°C) of the eight barrier polymer configurations and the uncoated configuration used.*

	Configuration number								
	1	**2**	**3**	**4**	**5**	**6**	**7**	**8**	**9**
First Layer	Barrier G	Barrier B	Barrier E	Barrier B	Barrier F	Barrier C	Barrier A	Barrier D	None
Second Layer	Barrier G	Barrier D	Barrier E	Barrier B	Barrier F	Barrier C	Barrier A	Barrier D	None
HVTR (g/m^2/h)	4.0	6.0	8.6	10.2	12.6	14.6	24.6	50.5	136.4
DiBP Migration (%)	7.1	7.1	29.4	26.3	23.3	27.3	35.4	49.4	62.3
DBP Migration (%)	3.2	4.7	25.0	25.8	21.6	26.3	30.1	35.3	48.7

5.4 Effect of temperature on the properties of the Barrier D.

The permeability of gases and vapours through a polymer film is influenced by the crystallinity, free-volume and the orientation of the polymer chains and increases with temperature, the extent of which varies for different polymers.[63, 66] The effect of temperature on the permeability of Config 2 and Config 8 was evaluated. Only these two configurations were evaluated as they both contained Barrier D as the top layer of the configuration. As discussed in the previous section (5.3), Barrier D was the only barrier polymer that was in the glassy state during the HVTR test and in the rubbery state during the migration test due to its Tg = 50°C. It would have been expected that more DiBP and DBP would migrate through Config 2 and Config 8 into Tenax® at 60°C than at 23°C. This was however not the case. Table 5. shows the specific migration of DiBP and DBP through Config 2 and Config 8 at both 23°C and 60 °C. More DiBP and DBP migrated into Tenax® when Barrier D was in the glassy state (i.e. 23°C) in comparison to when Barrier D was in the rubbery state (i.e. 60°C). This is contradictory to what would be expected and further investigation into this contradictory behaviour is described below.

Table 5.6: Comparison of the specific migration of Config 2 and Config 8 at 23°C and 60°C.

Migration Time (days)	Migration Temperature (°C)	Barrier D State	Specific Migration (%)			
			Config 2		Config 8	
			DiBP	DBP	DiBP	DBP
28	23	Glassy	7.1	4.7	35.3	49.4
1	60	Rubbery	2.0	2.9	16.4	26.8

It is suspected that some structural property of the barrier polymer is altered when the migration test is performed at 60°C. Crystallisation of the barrier polymer at 60°C could have occurred. Kurek *et al.* [67] determined the crystallinity of polyethylene films that were exposed to temperature-dependent permeability measurements. It was found that the crystallinity of the films decreased with increased exposure temperature. This was accompanied by an increase in permeability. Similar findings were observed by a number of authors. [19, 36] Diffusion and adsorption phenomena occur in the amorphous phase of semi-crystalline polymers such as polyethylene. The crystalline portion increases the path length of the diffusing molecules. This inhibits polymer chain mobility in the amorphous phase due to immobilisation of the chain ends in the surrounding crystalline phase. [66] The highest permeability of the polyethylene film was observed above the melting point of 40°C, reducing the crystalline phase. The effective path length of the diffusing molecules was reduced. The mobility of the polymer chains also increased, leading to increased free volume. Gajdos *et al.* [19] studied the barrier properties of polypropylene and polyethylene films with respect to oxygen and nitrogen at different temperatures. The permeability and solubility coefficient of polypropylene displayed Arrhenius behaviour, but a deviation was observed for the diffusion coefficient. This indicated that the effect of temperature on diffusion was more complicated than expected and could have been due to a dual-mode adsorption model where the diffusion is dependent on both the free-volume theory and polymer-penetrant interaction.

In order to confirm whether Barrier D could have crystallised during the migration test at 60°C, the barrier polymer was analysed by differential scanning calorimetry (DSC). A film sample was dried in a similar manner as used in the coated paperboard sample preparation, and then annealed at 60°C for 24 hours to simulate the migration conditions used. For

comparative purposes, Figure 5.4 shows a typical DSC curve for a polymer that tends to crystallise upon heating.[68] DSC thermograms are shown in Figure 5.5 of Barrier D before (dashed line) and after (solid line) conditioning. The slight endothermic deviation observed at approximately 50°C corresponds to the glass transition temperature of the barrier polymer. No melting endotherm peak was observed in the DSC curve of the conditioned barrier polymer and the curves for both the unconditioned and conditioned samples were found to be similar. This shows that the elevated temperature did not visibly have an effect on the crystallinity of the barrier polymer as initially suspected and does not clarify the deviation in the migration behaviour at 23°C and 60°C.
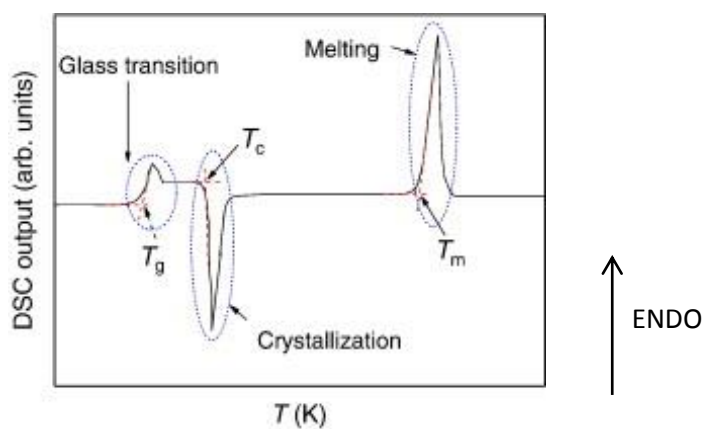

Figure 5.4: *Typical DSC curve of a polymer that crystallises during heating.[68]*
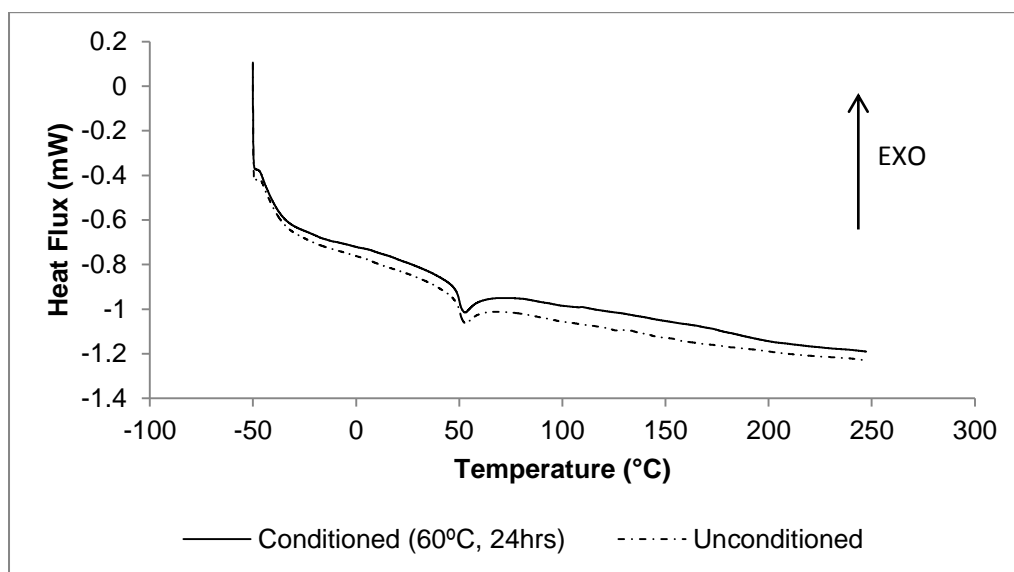

Figure 5.5: *The DSC trace of the barrier polymer, before and after conditioning.*

Another possible reason for deviation of Config 2 and Config 8 from the correlation between HVTR performed at 23°C and the specific migration performed at 60°C is a time factor. As mentioned previously, the testing time for the HVTR, specific migration at 60°C and the specific migration at 23°C are 1 h, 24 h and 28 days respectively.

5.5   Effect of the testing time on the correlation between HVTR and specific migration.

In order to compare the different polymers, the HVTR must have reached the steady state and the lag-time must be exceeded for the migration of DiBP and DBP to allow for measureable migration levels.

5.5.1   HVTR testing time.

The testing time for the HVTR test as defined by Tiggelman *et al.*[52] is one hour, provided that the steady state has been achieved. To confirm whether the eight coating configurations had in fact reached steady state during the one hour testing time, the HVTR test was extended to 3 hours and 7 hours. Figure 5.6 and Table 5.7 shows the HVTR results for the eight coating configurations for the different testing times. All results were normalised to one hour. The steady state is reached when the normalised HVTR value no longer changes significantly over time. Config's 1, 2 and 7 reached the steady state after one hour and Config's 3, 4, 5 and 6 reached steady state after three hours. Only Config 8, which is a double-layer configuration of Barrier D that has a glass transition temperature of 40°C, did not reach steady state after seven hours. This shows that the initial testing time of 1 hour was not sufficient to ensure that all eight coating configurations had reached steady state. If the HVTR test is to be used as an indicator for specific migration on a production scale, a single testing time for HVTR will be needed. The HVTR testing time was further extended to 24 hours as an attempt to ensure that the steady state had been reached for all eight coating configurations. Unfortunately, the paperboard samples became soiled by the uptake of heptane over the extended time period, making the determination of the HVTR inaccurate. No further attempts were made to determine the point where steady state was reached for all the configurations. It had already been shown that the original 1 h testing time was not adequate for all the configurations.
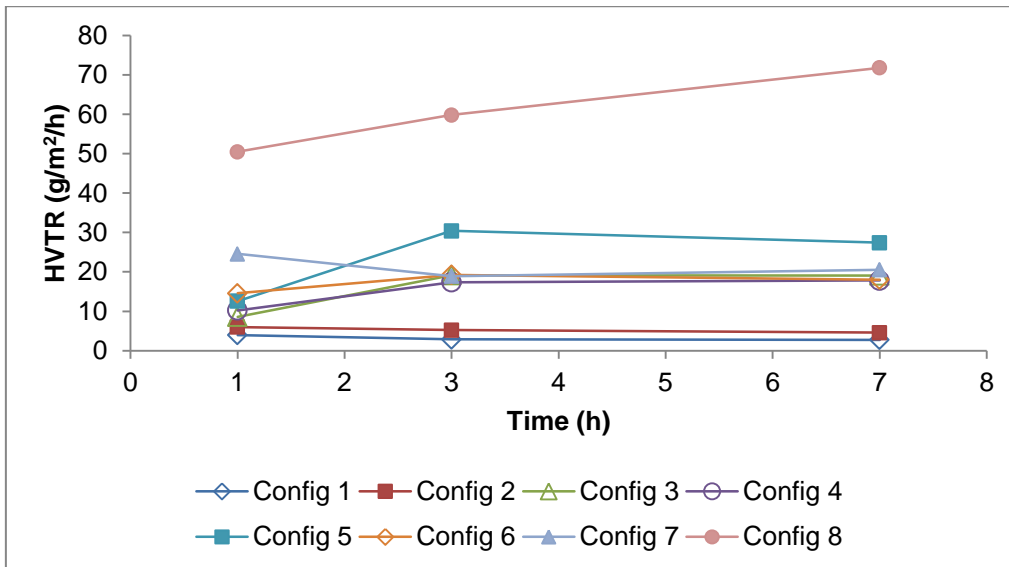
Figure 5.6: *Effect of testing time on the HVTR measured in g/m²/h.*

Table 5.7: Effect of testing time on the HVTR measured in g/m²/h.

Testing time (h)	1	3	7
Configuration number	HVTR (g/m²/h)		
1	4.0	2.9	2.7
2	6.0	5.3	4.6
3	8.6	19.2	19.1
4	10.2	17.4	17.8
5	12.6	30.4	27.4
6	14.6	19.2	18.0
7	24.6	18.9	20.6
8	50.5	59.8	71.8
9	136.4	97.3	71.3

5.5.2 Specific migration testing time

Two factors need to be taken into consideration for the testing time of the specific migration test for the eight coating configurations evaluated in this study. These are the lag-time and the migration equilibrium.

5.5.2.1 Lag-time or breakthrough

The lag-time or breakthrough time of a barrier film is defined as the time it takes for the chemical contaminant to migrate through the bulk of the barrier film to reach the interface between the barrier film surface and the food or food-simulant.[48] The barrier efficiency of the different polymers used in this study may have different lag-times. It is therefore necessary to choose a testing time period where the lag-time is exceeded for all the barrier configurations.

The testing time for the specific migration test was extended from 1 day at 60°C to 3, 7 and 10 days at 60°C in order to determine at what point breakthrough is observed. Figure 5.7 and Figure 5.8 shows the migration of DiBP and DBP as a function of time up to 3 days for the eight coating configurations. The data was plotted in this manner in order to accentuate the point of breakthrough. All of the coating configurations show breakthrough after 1 day, except Config 2 that only shows partial breakthrough. This would explain why Config 2 deviates from the initial correlation between the specific migration of DiBP and DBP at 60°C for 1 day and HVTR at 23°C (Figure 5.2).
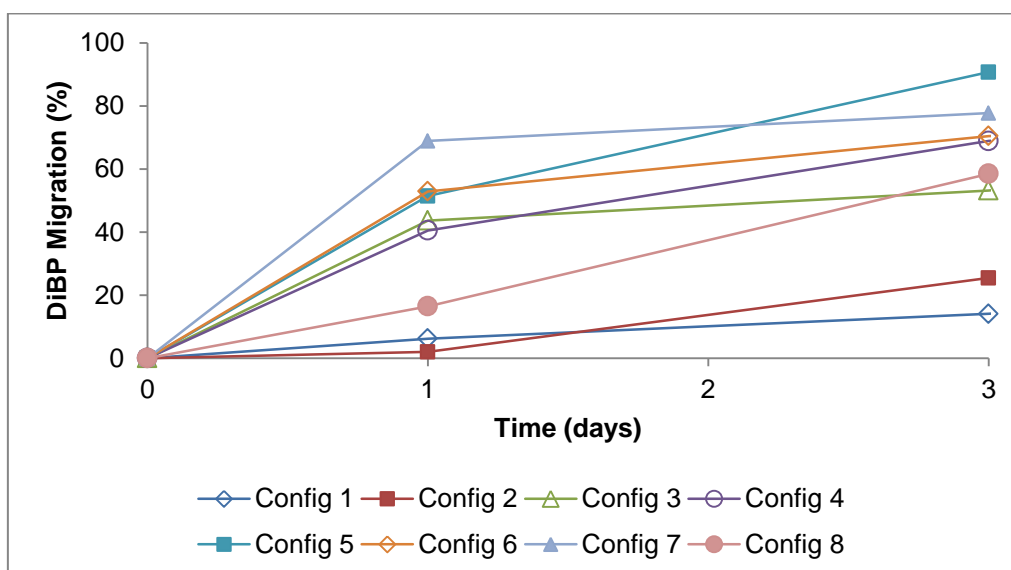
Figure 5.7: *Determination of breakthrough point for the migration of DiBP over time.*
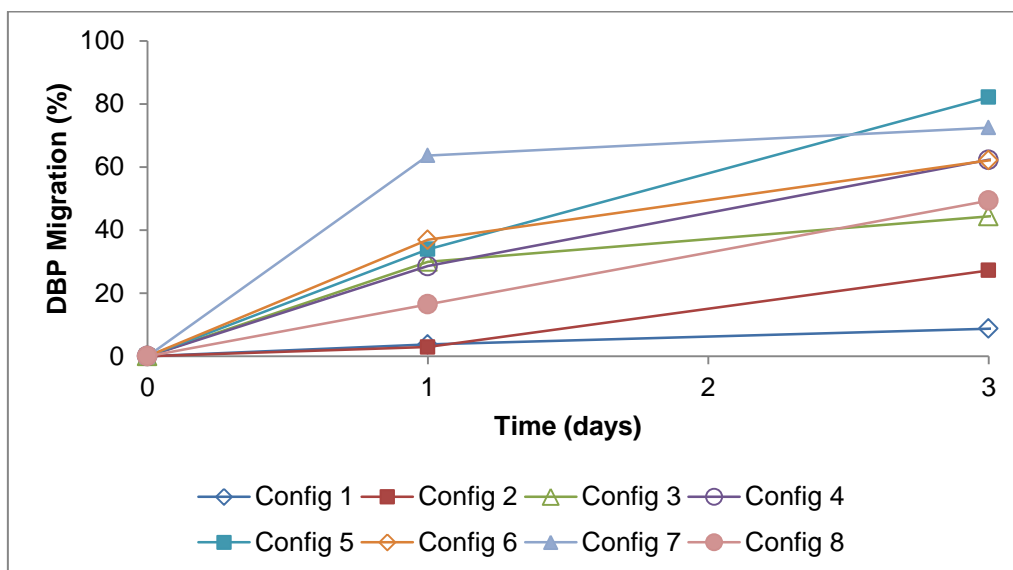
Figure 5.8: *Determination of breakthrough point for the migration of DBP over time.*

5.5.2.2   Migration equilibrium

The next point to consider is whether or not migration equilibrium is reached for all eight coating configurations during the testing period selected. The migration equilibrium is the maximum amount of a chemical contaminant that will migrate through the barrier film into Tenax®. In order to determine the migration equilibrium, a migration experiment should be conducted for an extended period of time, where the concentration of the chemical contaminant that has migrated into the food simulant is being determined periodically. The plot of the concentration vs. time will increase until the migration equilibrium is reached. Thereafter, no change in concentration should be observed with time.

To determine whether or not the eight coating configurations have reached the migration equilibrium within the 1 day testing period selected, the testing period was extended to 3, 7 and 10 days. Figure 5.9, Figure 5.10 and Table 5.8 shows the percentage migration of DiBP and DBP as a function of time for the eight configurations. Config 3, 4, 6 and 7 initially show rapid migration after 1 day, followed by a slight increase in the percentage migration until the migration equilibrium is reached at 7 days. Config 1, 2 and 8 show a gradual increase in the percentage migration over time until the migration equilibrium is reached after 7 days. Config 5 reaches its migration equilibrium after 3 days. Between 7 days and 10 days, a reduction in the percentage migration is observed. This is likely due to redistribution of DiBP and DBP from the Tenax® into the paperboard after the equilibrium migration is attained. Choi et al.[61] observed similar behaviour for the migration of DBP and benzophenone (BP)

57

from spiked paperboard through a polyethylene barrier into water. They attributed this behaviour to the volatility of DBP and BP and the subsequent loss into the headspace of the testing cell after the initial migration equilibrium was attained. Nerin et al.[32] also noted that Tenax® tends to release adsorbed chemical contaminants after extended exposure at high temperature by thermal degradation.

The initial correlation as depicted in Figure 5.2, is constructed using migration data for the eight different coating configurations after a testing time of 1 day. Even though none of the coating configurations have attained the migration equilibrium after 1 day, some configurations are closer to their migration equilibrium than others and show different migration rates. This could provide yet another explanation as to the deviation of Config 2 and Config 8 observed in Figure 5.2 and the subsequent adherance of these two configurations in Figure 5.3 when the migration testing time was extended to 28 days at room temperature.
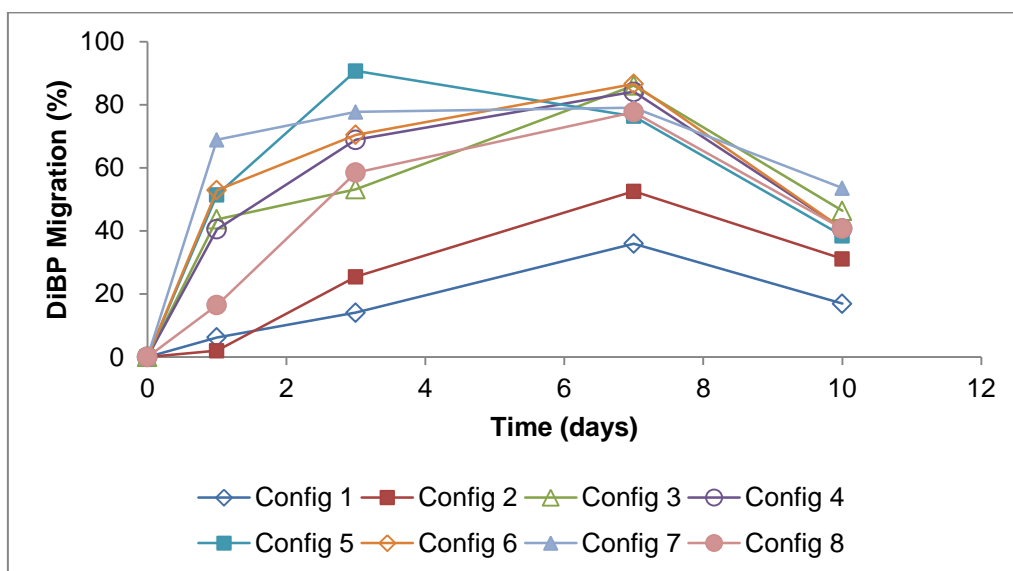
Figure 5.9: *The percentage migration of DiBP over time, for all coating configurations at 60°C.*
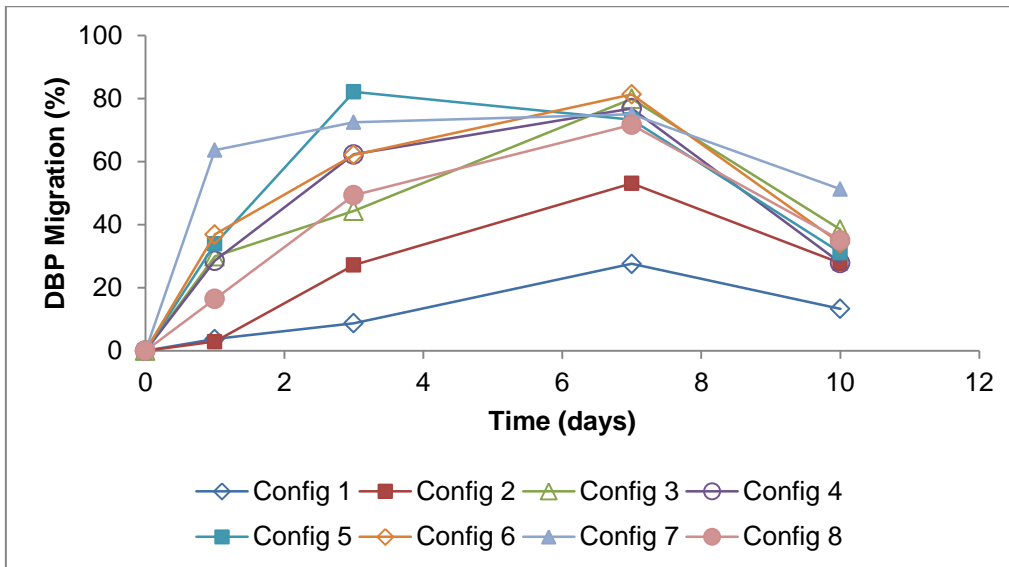
Figure 5.10: *The percentage migration of DBP over time for all coating configurations at 60°C.*

Table 5.8: *The percentage migration of DiBP and DBP over time for all coating configurations at 60°C.*

Contaminant	DiBP				DBP			
Testing time (days)	1	3	7	10	1	3	7	10
Configuration number	Migration (%)				Migration (%)			
1	6.2	14.1	35.9	16.9	3.7	8.7	27.5	13.3
2	2.0	25.5	52.5	31.1	3.0	27.2	53.1	27.8
3	44.0	53.2	86.1	46.4	30.0	44.4	79.9	38.4
4	41.0	68.9	84.1	40.7	29.0	62.3	76.8	27.9
5	51.0	90.7	76.3	38.4	34.0	82.1	73.3	31.1
6	53.0	70.5	86.6	40.7	37.0	62.1	81.3	34.1
7	69.0	77.7	79.0	53.6	64.0	72.5	75.0	51.3
8	16.0	58.5	77.6	40.7	16.0	49.4	71.7	35.1

5.6   Conclusion

The HVTR and the specific migration of a number of different barrier coating configurations were correlated in an attempt to produce a universal correlation that can be used for any type of barrier polymer.

The glass transition temperature of the polymer should be taken into consideration as well as the relation of the Tg to the HVTR and specific migration testing temperature. The barrier polymer must be in the same state at the conditions used to determine both the HVTR and the specific migration. It was seen that in the case of Barrier D, it was in the glassy state during the HVTR test at 23°C but in the rubbery state during the migration test at 60°C. Migration mechanisms of organic gases and vapours through barrier polymers are different in the glassy and rubbery states.

The testing time was also identified as an important variable to consider. The initial testing time selected for the HVTR (1 h) and the specific migration (1 day) were not sufficient to obtain comparable data for all eight coating configurations. In the case of the HVTR test, the eight different coating configurations reached steady state after different time intervals, with Barrier D not reaching steady state after 7 h. Performing the HVTR test for 24 h led to soiling of the samples. For the specific migration test, the lag time and the migration equilibrium need to be considered when selecting the testing time. Config 2 was the only coating configuration to show a lag time which was only exceeded after 3 days. The eight coating configurations reached the migration equilibrium at similar time intervals, but at different rates.

There are numerous properties of the barrier polymers and the testing conditions that will have an impact on the correlation between HVTR and specific migration. However, based on the three properties evaluated, namely the Tg of the barrier polymer, the testing temperature and the testing time, a universal correlation between HVTR and specific migration that is valid for any type of barrier polymer is not of practical applicability. It will rather be more applicable to establish a correlation between HVTR and specific migration for each type of barrier polymer to be used, which will be considered in the next section.

CHAPTER 6

CORRELATION BETWEEN HVTR AND SPECIFIC MIGRATION FOR A SPECIFIC BARRIER POLYMER

6.1   Introduction

In the previous chapter, it was shown that a universal correlation between HVTR and specific migration for any kind of barrier polymer appeared to not be possible. The migration of chemical contaminants through a barrier film is determined by a number of factors. These include the chemical nature of the chemical contaminant and the composition of the barrier film and its morphology. In order for the correlation between HVTR and specific migration to be of practical application, the correlation would need to be determined for each different type of barrier polymer to be used in paperboard packaging applications.

In order to construct the correlation between HVTR and the specific migration, the barrier properties of the individual barrier polymer needs to be varied. This was achieved by varying the thickness of the barrier polymer applied to the paperboard substrate.

6.2   Effect of barrier film thickness on the correlation between HVTR and specific migration

Two different barrier polymers were used. A PVDC-type barrier polymer was selected as it was identified as the best performing barrier polymer in the previous chapter. A styrene-acrylic type barrier polymer was also selected, as it is a commonly used barrier polymer in paperboard packaging applications.

Ten different coating configurations, ranging from 5 g/m^2 to 45 g/m^2 were prepared using grooved rods with increasing winding thickness. Single and double layer coating configurations were evaluated. The change in coating thickness is determined in terms of the coating weight.

Both of the barrier polymers selected have a Tg value lower than 23°C. Consequently, the polymers were in the rubbery state during both migration tests performed at 23°C and at 60°C. Migration of the chemical contaminants will therefore occur by the same mechanisms at both temperatures. It was also decided to rather perform the migration test at 60°C for 3 days instead of at 23°C for 28 days to speed up the experiments.

6.2.1 PVDC barrier polymer

The thickness of the barrier film was varied by using coating rods with varied winding thickness as well as by preparing single-layer and double-layer configurations. The film thickness was measured indirectly by determining the coating weight of the barrier film.

The effect of the change in coating weight on HVTR and specific migration was evaluated. The testing time for the HVTR test was extended from one hour to three hours as it was shown earlier that this particular polymer reached a steady state after 3 hours (see 5.5.1). The HVTR result obtained after the three hours testing time was normalised to one hour.

Figure 6.1 and Table 6.1 show the change in the HVTR as a function of coating weight. The configuration with the lowest applied coating thickness (6 g/m^2) gave a corresponding HVTR of 22 g/m^2/h. This point was however excluded from Figure 6.1 so as not to suppress the trend of the remaining configurations that all have HVTR values below 10 g/m^2/h. There was an initial reduction in the HVTR as the coating weight increases from 5 g/m^2 to 23 g/m^2. No further reduction in HVTR was observed for coating weights exceeding 23 g/m^2.
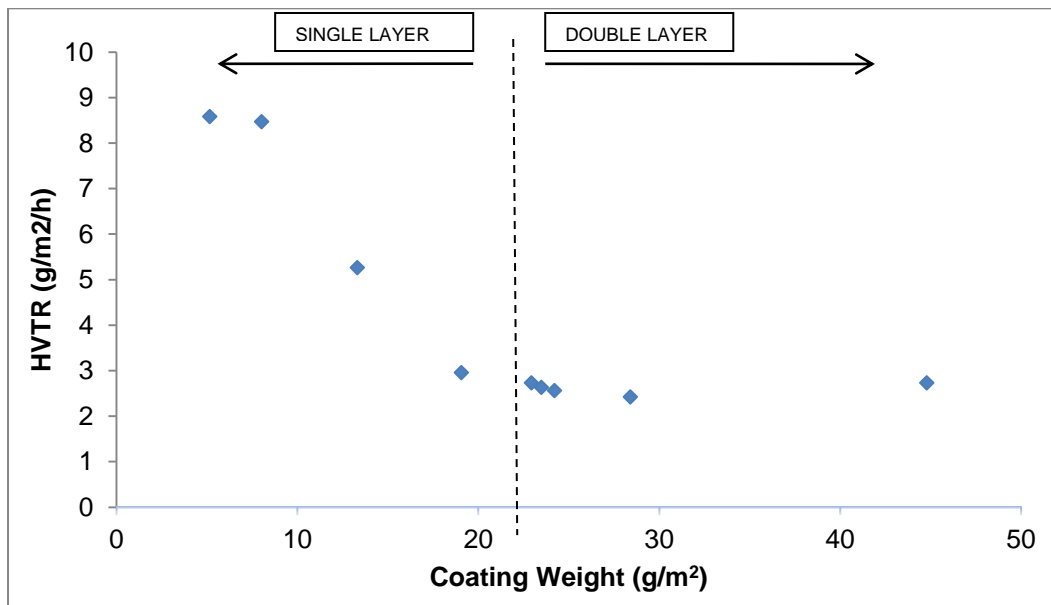
Figure 6.1: *HVTR as a function of coating weight for the PVDC barrier polymer.*

Table 6.1: *Coating weight and HVTR data for the PVDC barrier polymer.*

Coating weight (g/m^2)	HVTR (g/m^2/h)
6	22.7
5	8.6
8	8.5
13	5.3
23	2.7
19	3.0
23	2.6
24	2.6
28	2.4
45	2.7

Weiss[26, 69] observed similar behaviour in polymer films that were coated with aluminium by vacuum vaporisation. The thickness of the aluminium coating was varied and was monitored as a change in the optical density. The optical density increased as the film thickness was increased. Figure 6.2 shows the relationship observed between the oxygen and water vapour transmission and the optical density of the aluminium coated polymer films. An initial decrease was observed in both the oxygen and the water vapour transmission rate up to a particular optical density. The transmission rates became independent of optical density above the particular optical density. The change in transmission rates below the particular optical density was attributed to the presence of pinholes. This type of behaviour has also been attributed to the minimum amount of coating required for complete coverage of the substrate.[26]
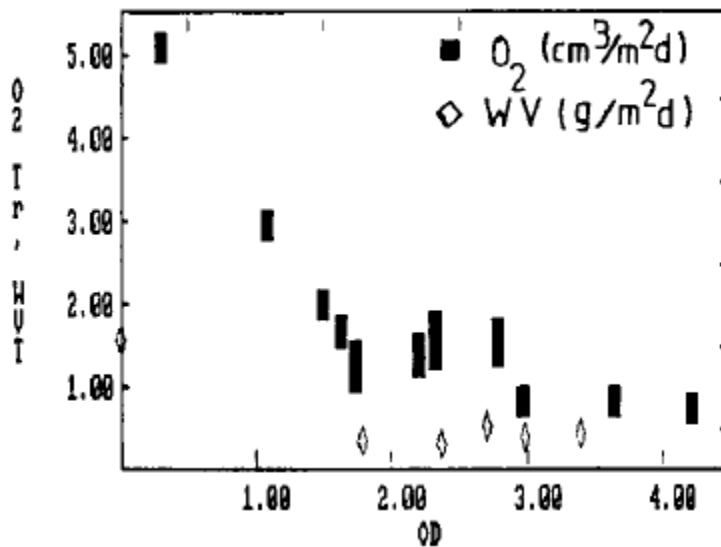
Figure 6.2: *Dependence of oxygen and water vapour transmission on optical density.*[69]

In this work, the coating weights above 23 g/m^2 correspond to double-layer coatings. The double-layer coating would ensure complete coverage of the paperboard substrate and cover up any defects present in the first layer. To confirm this, a surface defect test was performed. Methanol was applied to the surface of coated paperboard (10 cm x 10 cm) and inspected visually for defects. Surface defects such as cracks and pinholes will appear as darkened areas on the surface. Figure 6.3 shows images of the surface defect test for the single-layer configurations and one double layer configuration. The first single-layer configuration with a coating weight of 6 g/m^2 showed a significant number of pinholes and poor coverage of the paperboard substrate. This clarifies the high HVTR value (22 g/m^2/h) observed in comparison to the second configuration that has a similar coating weight (5 g/m^2). Numerous defects were observed for the single-layer configurations, with a consistent decrease in pinhole density as the coating weight increased. No surface defects were observed for the double-layer configurations.
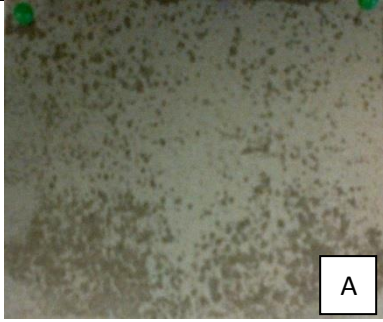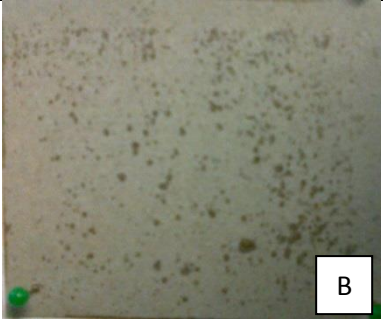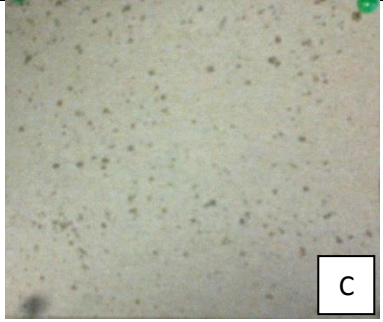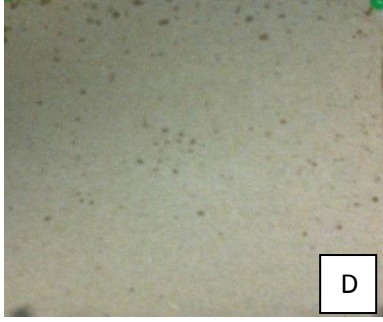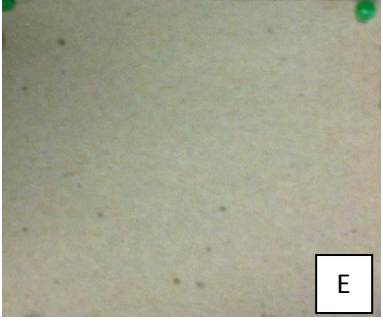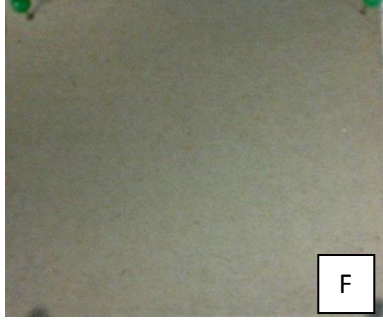
First Single-layer configuration Coating weight = 6 g/m^2	Single-layer configuration Coating weight = 5 g/m^2	Single-layer configuration Coating weight = 8 g/m^2
Single-layer configuration Coating weight = 13 g/m^2	Single-layer configuration Coating weight = 23 g/m^2	Double-layer configuration Coating weight = 45 g/m^2

Figure 6.3: Surface defect test. Five single layer configurations and a double layer configuration are shown.

In order to determine whether a relationship exists between the number of pinholes and the HVTR, the number of pinholes present on the surface of the single-layer configurations was quantified. The number of pinholes or the pinhole density is determined by applying a grid composed of 100 blocks to the image of the single-layer configurations captured during the surface defect test. The number of blocks in the grid occupied by a pinhole(s) are counted and expressed as a percentage. Figure 6.4 and Table 6.2 shows the relationship between the pinhole density (PD) and the HVTR of the single-layer configurations, with the coating weights for each configuration included on the graph. The HVTR decreases as the pinhole density decreases and the coating weight increases.
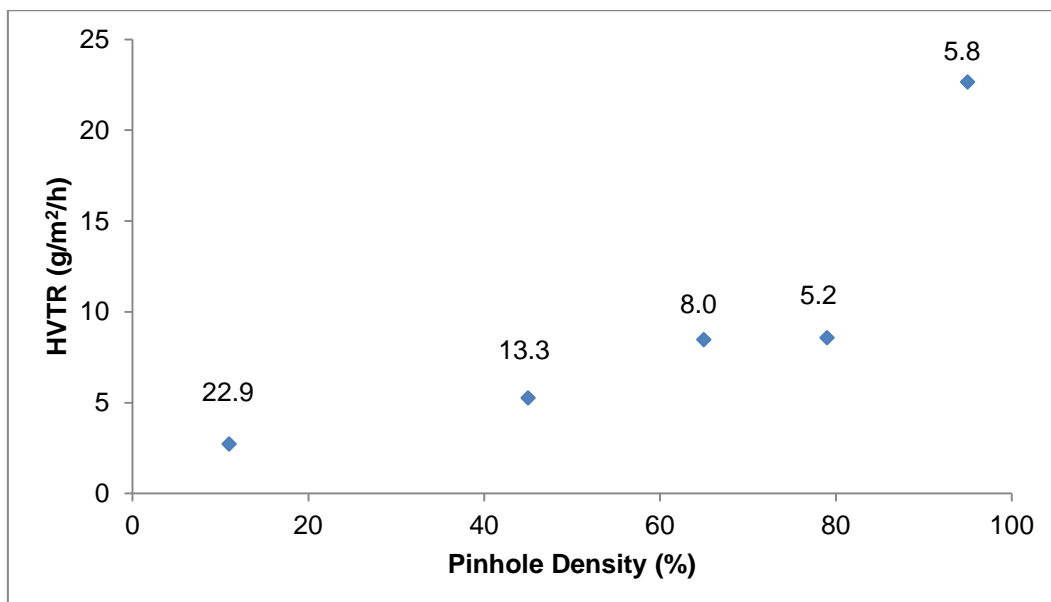
Figure 6.4: *Relationship between the pinhole density and HVTR for the single-layer PVDC configurations. The coating weights for each configuration are included as data labels above each point on the graph.*

Table 6.2: *Relationship between pinhole density, HVTR and coating weight for the PVDC polymer.*

Configuration number	Coating weight (g/m^2)	HVTR (g/m^2/h)	Pinhole density (%)
1	6	22.7	95
2	5	8.6	79
3	8	8.5	65
4	13	5.3	45
5	23	2.7	11

There are two models that can be used to describe the transport of gases and vapours through a barrier film (See 2.4.4). The defect model is dependent on presence of pinholes or surface defects, whereas the solution-diffusion model is dependent on the coating thickness.[26] Upon initial inspection, the transport properties for the HVTR test appeared to be

best described by the defect model. The HVTR decreased as the pinhole density decreased (single-layer coatings) and remained constant regardless of coating weight when no pinholes were present (double-layer coatings). However, in the case of the single-layer coatings, both the pinhole density and the coating weight varied and therefore either transport model could apply. To confirm the transport model for the single-layer coatings, coating configurations were prepared where the coating weight was kept constant and the pinhole density was varied. The pinhole density was varied by subjecting the PVDC barrier polymer to high shear mixing for different time intervals to incorporate air into the coating. In this case, the coating was subjected to a shear rate of 1300 rpm for 0, 1, 5, 7, and 10 min. The coating was applied to the paperboard surface (average of 29 g/m^2) and allowed to dry. The coating weights applied are shown in Table 6.3. Upon drying, pinholes formed upon rupture of the air bubbles.

Figure 6.5 shows the effect of the pinhole density on the HVTR. The HVTR value increases as the pinhole density increases. The coating weight for each configuration is similar as calculated the Student's t test (see Table 6.4). This confirms that the transport mechanism for the HVTR test conforms to the defect model and is controlled by the presence of pinholes on the film surface and is independent of film thickness. This correlation will also allow the estimation of the pinhole density based on the measurement of the HVTR.
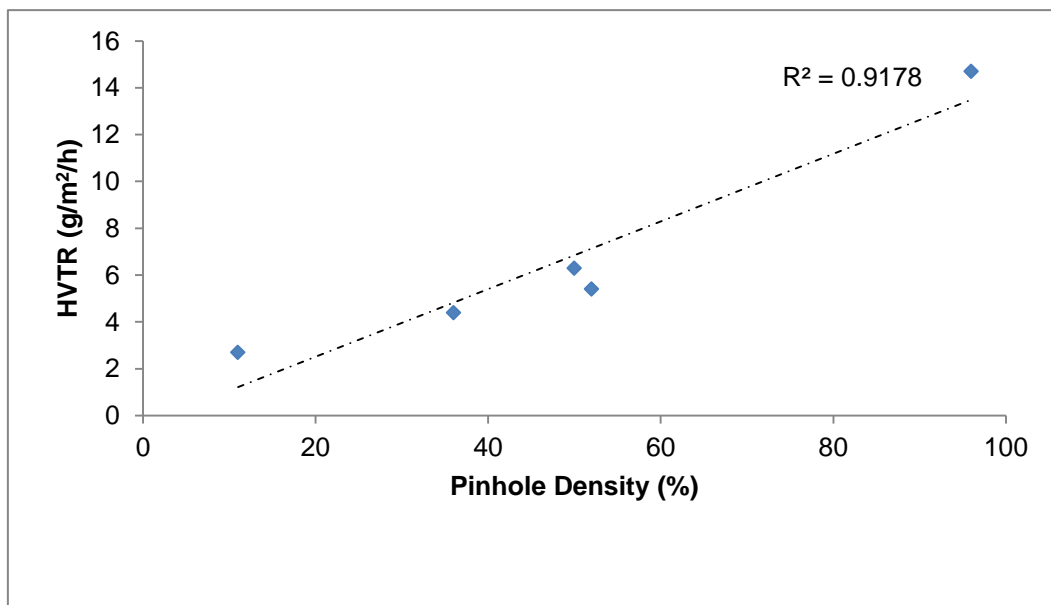
Figure 6.5: *The effect of pinhole density on HVTR where the coating weight (29 g/m^2) is kept constant.*

$$PD(\%) = \frac{HVTR + 0.3789}{0.1445}$$

Equation 6.1

Table 6.3: *Coating weight of PVDC barrier polymer with varied pinhole density.*

Shear time (min)	Coating weight (g/m²)	HVTR (g/m²/h)	Specific Migration (%)		Pinhole density (%)
			DiBP	DBP	
0	22.7	2.7	24.9	16	11
1	24.8	4.4	22.5	15.9	36
5	30.5	6.3	23.1	15.8	50
7	27.2	5.4	19.9	13.7	52
10	34.1	14.7	29.7	18.7	96

Table 6.4: *Student's t test comparing the average coating weight to the coating weight for the individual shearing times.*

Shearing time (min)	$T_{crit} = \pm 12.7$ (95% confidence, 1 degree of freedom)	
	T_{stat}	$T_{crit} > T_{stat}$
0	-9.7	✓
1	-2.3	✓
5	0.6	✓
7	-0.1	✓
10	1.0	✓

The same coating configurations used in the HVTR evaluation were also used to evaluate the specific migration of DiBP and DBP. The specific migration test was performed for three days as this is sufficient time to overcome the lag-time as shown in the previous chapter (5.5.2.1). Figure 6.6 and Table 6.3 shows the relationship between the pinhole density and the percentage specific migration of DiBP and DBP. The specific migration of DiBP and DBP did not change significantly up to a pinhole density of about 50%. Only a slight increase in specific migration was observed for the highest pinhole density (i.e. 95%). The increase in the specific migration at the highest pinhole density was most likely due to the size and distribution of the pinholes on the sample surface that results in insufficient surface coverage. Figure 6.7 shows images of the surface defect test for pinhole densities of 11%, 50% and 96%. This shows the poor surface coverage observed for the sample with a pinhole density of 96% in comparison to the samples with lower pinhole densities. This confirms that the defect model does not apply to the specific migration of DiBP and DBP. The specific migration is rather controlled by the diffusive-flow mechanism where the transport mechanism is dependent on the coating weight or thickness and independent of surface defects.
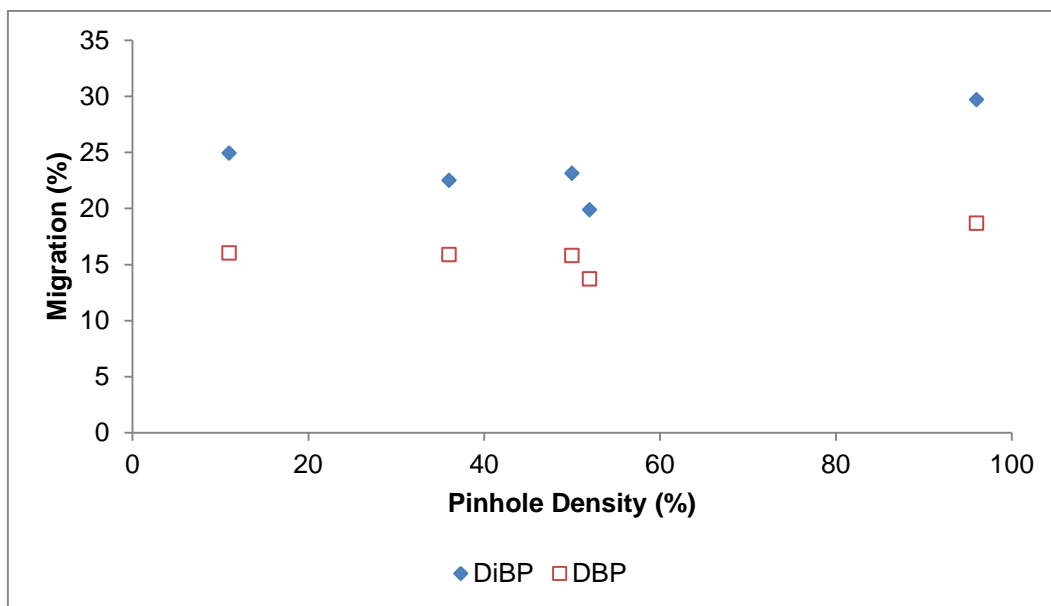
Figure 6.6: *The effect of pinhole density on the specific migration of DiBP and DBP where the coating weight is kept constant.*

| Pinhole density = 11% | Pinhole density = 50% | Pinhole density = 96% |
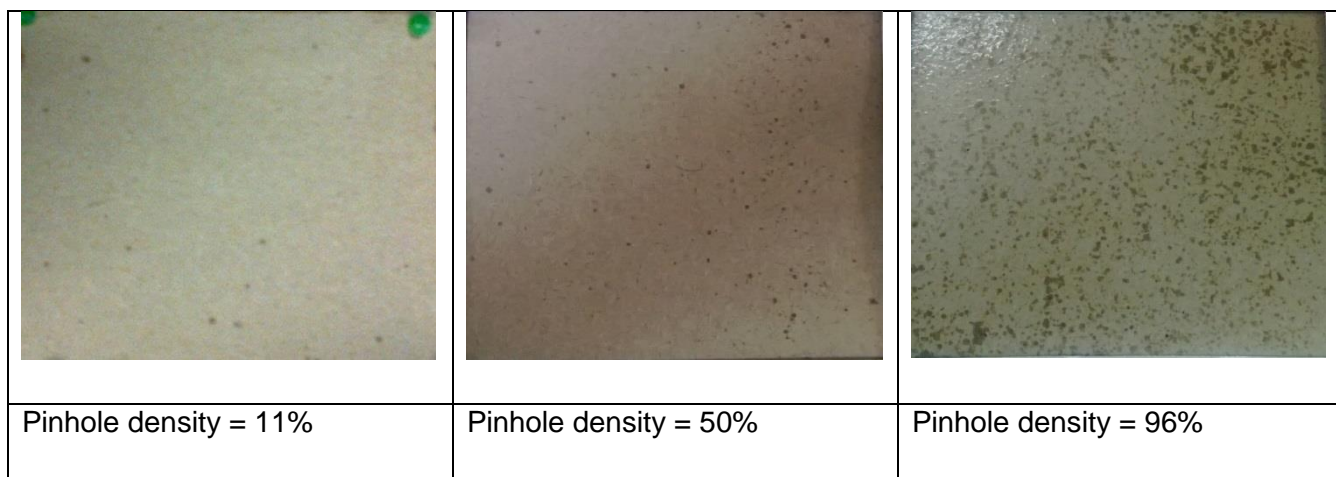
Figure 6.7: *Surface defect test. Pinhole densities of 11%, 50% and 96% are shown.*

The above results show that the transport mechanism for the HVTR test and the specific migration test are different. Thus, a direct correlation will not be feasible.

6.2.2 Styrene-acrylic barrier polymer

The same testing conditions were used for the styrene-acrylic barrier polymer as were used for the PVDC polymer. The HVTR was extended to 3 h at 23°C and the migration test was extended to 3 days at 60°C. Figure 6.8 shows the change in the HVTR as a function of coating weight while Figure 6.9 shows the change in the specific migration of DiBP and DBP as a function of coating weight. The double-layer coating configuration with the greatest coating weight was excluded from the HVTR and specific migration analysis. This was due to the fact that the coated surface was tacky and was damaged during the spiking stage of the sample preparation.

Both the HVTR and the specific migration show no significant change as the coating weight is increased. This particular barrier polymer presents a poor barrier to migration as the migration of both DiBP and DBP through the barrier polymer into the Tenax is close to 100%.
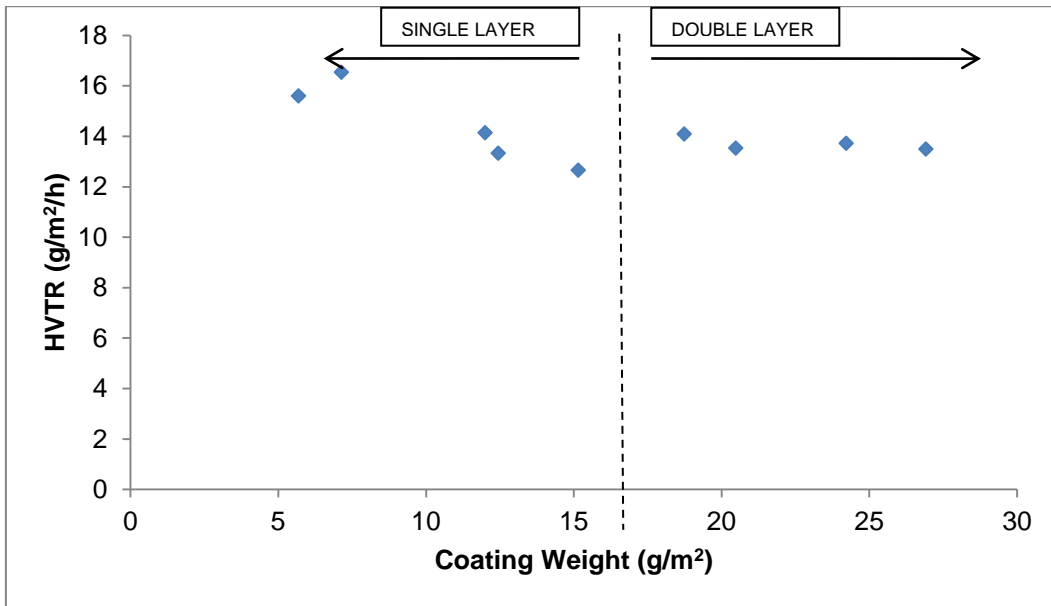
Figure 6.8: *HVTR as a function of coating weight for the styrene-acrylic barrier polymer.*
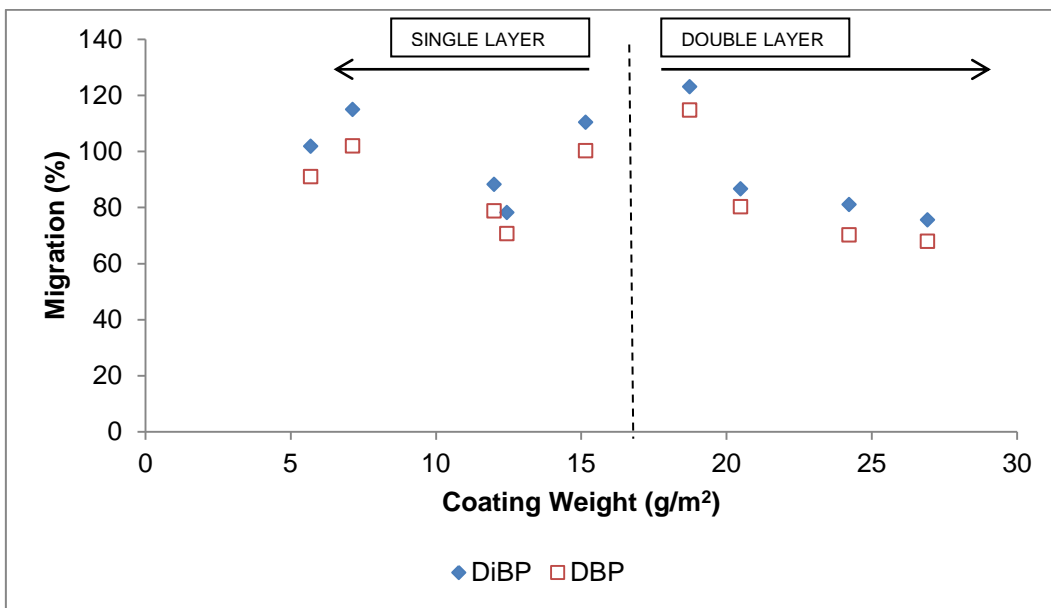
Figure 6.9: *Migration of DiBP and DBP as a function of coating weight for the styrene-acrylic barrier polymer*

Table 6.5*: Coating weight, HVTR and specific migration data for the styrene-acrylic barrier polymer.*

Coating weight (g/m^2)	HVTR (g/m^2/h)	Specific migration (%)	
		DiBP	DBP
7	17	115	102
12	14	88	79
6	16	102	91
15	13	110	100
20	14	87	80
12	13	78	71
19	14	123	115
24	14	81	70
27	14	76	68

6.3 The correlation between HVTR and specific migration of DiBP and DBP for the PVDC barrier polymer

The transport mechanisms for the HVTR test and the specific migration test are different, making a direct correlation between the two implausible. However, an indirect correlation is possible. The HVTR can give an indication of film integrity as the transport mechanism is dependent on pinholes. The specific migration can be estimated by monitoring the coating weight as the transport mechanism is dependent on coating weight.

6.3.1 HVTR as a function of film integrity

The HVTR test is a simple and rapid method that can easily be implemented in quality control laboratories with minimal start-up cost and level of operator expertise. The HVTR of barrier coated paperboard can be monitored on an on-going basis during paperboard production as an indicator of the presence of pinholes. With particular reference to the PVDC

barrier coating evaluated in this study and using Figure 6.1, three HVTR limits are identified that can be used to assess the film integrity exclusive of this PVDC barrier coating.

a) HVTR < 3.0 g/m²/h - The coated surface is free of pinholes.

b) 3.0 g/m²/h < HVTR < 10 g/m²/h - Pinholes are present on the coated surface. However the presence of the pinholes will not have an influence on the barrier to specific migration.

c) HVTR > 10 g/m²/h - The film integrity is poor and the barrier properties to the specific migration will deteriorate.

These limits will need to be identified for each type of barrier polymer used for paperboard packaging applications.

6.3.2 *Specific migration as a function of coating weight*

The specific migration is dependent on the coating weight, irrespective of the presence of pinholes, provided the HVTR is less than 10 g/m²/h for this particular PVDC barrier polymer. It is therefore possible to construct a correlation between the coating weight and the percentage specific migration that can be used on a production scale. Figure 6.10 shows the correlation between the coating weight and the percentage specific migration of DiBP and DBP for the single-layer and double-layer PVDC configurations. A linear correlation is observed between the percentage specific migration and the coating weight as the correlation coefficient, R^2, for both DiBP and DBP exceeds $R^2 = 0.8$ which is considered to indicate a strong linear correlation.[64] The equations of the linear trend lines are shown below. These equations can be used to estimate the percentage specific migration based on the coating weights determined during production of coated paperboard for packaging applications.

$$\%Migration_{(DiBP)} = (-0.5919 \times CW) + 36.816 \qquad \text{Equation 6.2}$$

$$\%Migration_{(DBP)} = (-0.5253 \times CW) + 28.946 \qquad \text{Equation 6.3}$$

It is important to note that monitoring the coating weight and the use of the above correlation will give an indication of the percentage specific migration. In order to determine the actual

specific migration that can be expected, the quantity of DiBP and DBP present in the paperboard will need to be determined. This can easily be done by extracting the paperboard in the appropriate solvent, followed by quantification by GC-MS.
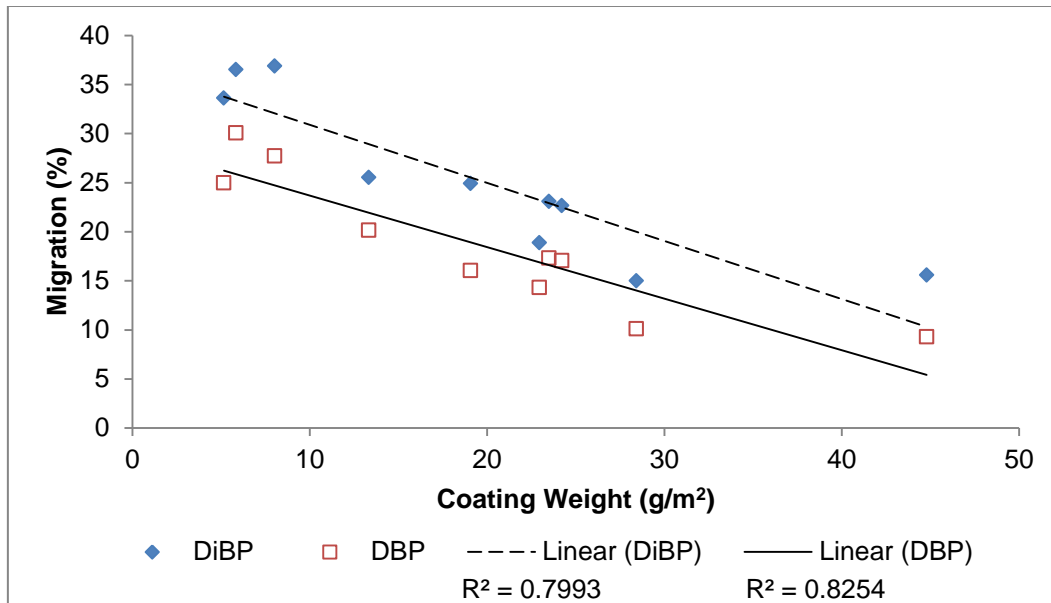
Figure 6.10: *Correlation between coating weight and the specific migration of DiBP and DBP for the PVDC barrier polymer.*

6.3.3 Prediction of migration within product shelf-life

The above correlation makes it possible to determine the specific migration of DiBP and DBP from PVDC-coated paperboard packaging into a food simulant under specific exposure conditions. However, the correlation was constructed under accelerated laboratory conditions that would need to be related to commercial conditions of use.

The Arrhenius equation can be used to calculate the contact time under commercial conditions relative to the accelerated conditions used. [18, 48]

$$t_1 = \frac{t_2}{e^{\left[\frac{-Ea}{R} \times \left(\frac{1}{T_1} - \frac{1}{T_2}\right)\right]}}$$

Equation 6.4

Where t_1 is the actual contact time, t_2 is the accelerated testing time, E_a is the activation energy (*J/mol*), R is the gas constant (*8.31 J/K/mol*), T_1 and T_2 are the temperatures (K) of actual use and accelerated use, respectively. Using a worst case assumption for the activation energy of 80 000 J/mol [18] and the accelerated conditions used in this study (3 days at 60°C), the contact time at a given temperature of exposure necessary to achieve a migration level equivalent to the accelerated migration test can be calculated. Figure 6.11 shows the actual contact time of the PVDC coated paperboard as a function of actual usage temperatures. The equation of the curve in Figure 6.11 can then be used to calculate the actual contact time that the accelerated conditions represent for a specific usage temperature.
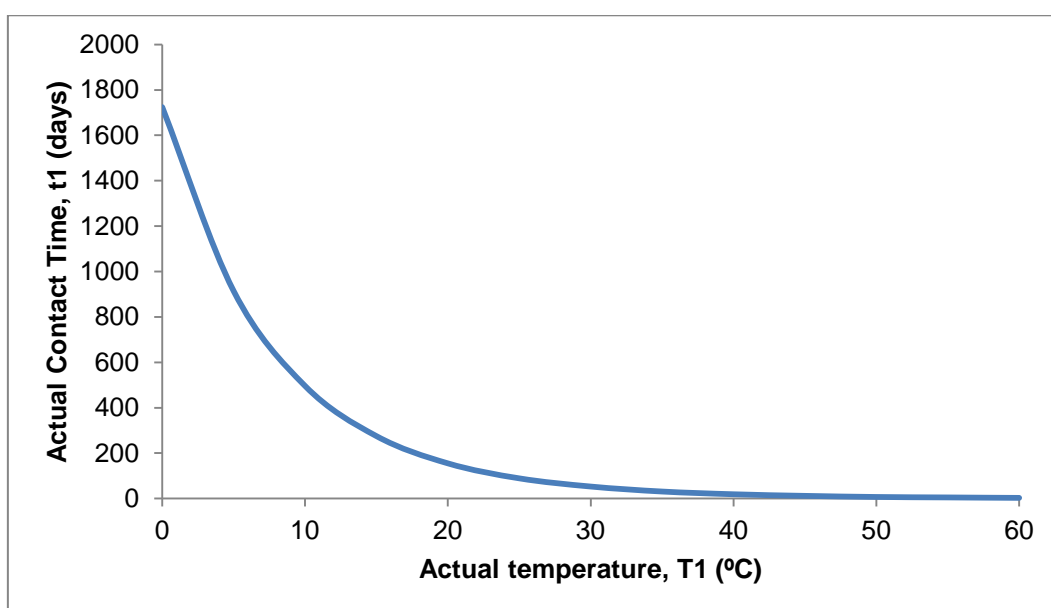
Figure 6.11: *Relationship between the actual contact time and usage temperature relative to the accelerated conditions of 3 days at 60°C used in this study.*

$$t_1 = 1572.7e^{(-0.1333 \times T_1)}$$

Equation 6.5

To illustrate the use of the specific migration vs. coating weight correlation, paperboard packaging for breakfast cereals was used as an example. This type of product is normally stored at room temperature i.e. 23°C. The correlation would thus be able to predict the effectiveness of the PVDC barrier to retard the specific migration of DiBP and DBP from the paperboard into the breakfast cereal for a contact time of 111 days at 23°C. A hypothetical

paperboard sample coated with the PVDC barrier polymer has a coating weight of 10 g/m^2 and contains 75 $\mu g/dm^2$ each of DiBP and DBP. Using the correlation shown in Figure 6.10, the percentage migration, actual migration and the conformance to the SML of DiBP and DBP were calculated and are shown in Table 6.

Table 6.6: *Calculation of the actual specific migration of DiBP and DBP using the proposed correlation for a hypothetical sample with a coating weight of 10 g/m^2.*

Chemical Contaminant	Migration (%)	Migration ($\mu g/dm^2$)	SML ($\mu g/dm^2$)	Conformance to SML
DiBP	31	23.3	50	PASS
DBP	24	18.0	50	PASS

This shows that for a period of 111 days at 23°C, the specific migration of DiBP and DBP from the hypothetical PVDC coated paperboard sample into the breakfast cereal will be below the SML. However, breakfast cereals commonly have a shelf-life of 1 year. In order for the correlation to predict the specific migration of DiBP and DBP from the PVDC coated paperboard into the breakfast cereal for a period of 1 year, the testing conditions used to construct the correlation would need to be adapted to 60°C for 10 days as calculated using Equation 6.6.

$$t_2 = t_1 e^{\left[\frac{-Ea}{R} \times \left(\frac{1}{T_1} - \frac{1}{T_2} \right) \right]}$$

Equation 6.6

It should be noted that the EU Regulation 10/2011[18] states that 10 days is the maximum time period that may be used during accelerated testing. It is there important to take the final application of the product into consideration when constructing the correlation in order to select the correct accelerated conditions for the product shelf-life.

6.3.4 Validation

The concentration of the chemical contaminant present in the paperboard has an effect on the amount of migration through the barrier film.[63] The spiking level used in this study is selected to be twenty times the legal migration limit to ensure that measureable migration is observed. However, in commercial applications, the levels of these chemical contaminants present in the paperboard should be significantly lower than the legal migration limits.

In order to evaluate the effect of the DiBP and DBP concentrations present in the paperboard on the amount of migration through the PVDC film, the spiking concentration was reduced to a half and a quarter of the original spiking level. The migration test was performed at 60°C for 3 days. Figure 6.12 and Table 6.7 shows the change in the percentage specific migration of DiBP and DBP as a function of spiking level for the PVDC film with a coating weight of 8.0 g/m^2. The percentage specific migration of DiBP and DBP decreases as the spiking level is decreased and a linear correlation is observed. The correlation coefficient for both DiBP and DBP exceeds $R^2 = 0.8$ which is considered to indicate a strong linear correlation.[64]
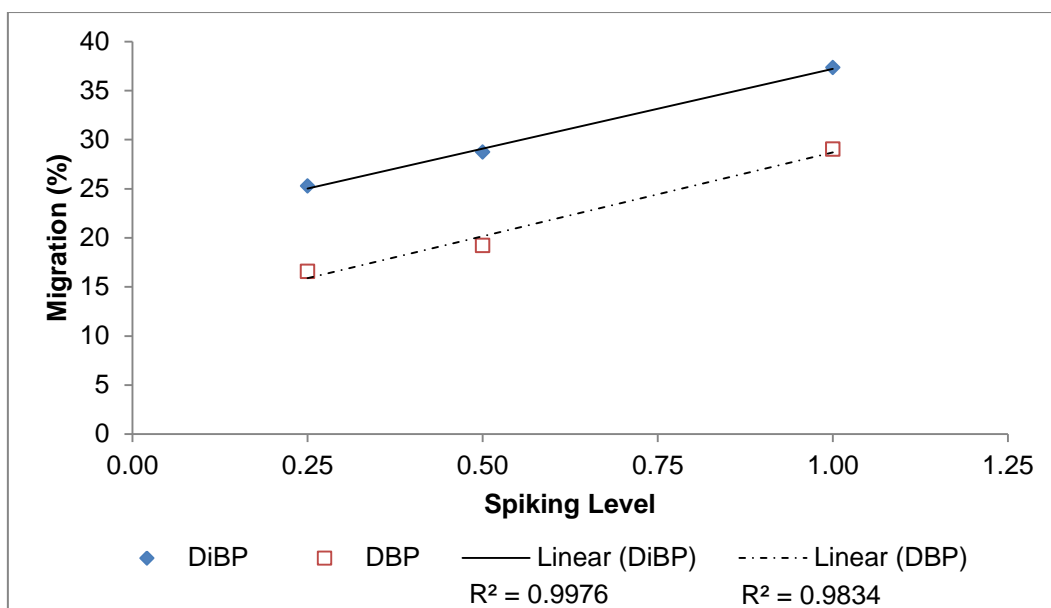

Figure 6.12: Effect of the spiking level on the specific migration of DiBP and DBP for a barrier film with a coating weight = 8.0 g/m^2.

Table 6.7: *Specific migration of DiBP and DBP through the PVDC barrier polymer as a function of spiking level.*

Spiking level	Specific migration (%)	
	DiBP	**DBP**
0.25	25	17
0.50	29	19
1.00	37	29

This shows that the percentage specific migration of DiBP and DBP through the PVDC film will decrease as the concentration of these compounds present in the paperboard decreases. Commercial samples contain significantly lower concentrations of DiBP and DBP in comparison to the spiked samples. When the proposed correlation between coating weight and the percentage specific migration is applied to commercial samples, the proposed correlation will over-estimate the percentage specific migration of DiBP and DBP for a specific coating weight.

6.4   Conclusion

The transport of volatile organic vapours and gases through thin barrier films can occur via two mechanisms. In the case of the HVTR test, the defect model applies, whereas in the case of the specific migration the diffusive flow model applies. Therefore a direct correlation between HVTR and specific migration is not plausible. However, an indirect correlation is possible. The HVTR can be monitored on a production-scale as an indicator of film integrity. Once it has been determined that the HVTR falls below a specific value, the coating weight of the coated paperboard product can be used to calculate the percentage specific migration. It is important to note that each type of chemical contaminant and barrier polymer will have a unique correlation equation that must be used to calculate its percentage specific migration through the barrier polymer.

The Arrhenius equation was used to relate the constructed correlation to commercial usage conditions. It is important however to take the actual conditions of use into consideration before constructing the correlation. This will ensure that the correct accelerated conditions are selected in relation to the actual usage conditions.

The correlation was found to over-estimate the percentage specific migration for commercial samples due to the high spiking levels used in this study.

The nature of the barrier polymer was once again shown to result in very different barrier properties. The PVDC barrier polymer showed a percentage specific migration of 40% and 30% for DiBP and DBP respectively for the "worst-case" scenario. On the other hand, the styrene-acrylic barrier polymer provided poor barrier property. The relationship between HVTR, coating weight and percentage specific migration will need to be determined for each type of barrier polymer used in paperboard packaging applications.

CHAPTER 7

CONCLUSION AND RECOMMENDATIONS

7.1   Conclusion

Recycled paperboard is used as a fibre source for the production of paperboard for food packaging applications. The components constituting recycled paperboard are varied, which introduces uncertainty in terms of the chemical contaminants it contains. These chemical contaminants can potentially migrate into the packaged food, posing a significant health concern for the end user.

The aim of this study was to correlate the permeation method (HVTR test, a simplified permeation test method using heptane as a permeant) to the actual migration levels of specific contaminants, in particular DiBP, DBP and DEHP. The first phase of the study focussed on establishing a universal correlation between the HVTR and the specific migration of DiBP, DBP and DEHP that would be applicable to any type of functional barrier. Experimental data demonstrated that the correlation factor relating HVTR to specific migration levels was largely dependent on the type and morphology of the barrier polymer considered. This work thus demonstrated that such a universal correlation does not appear to exist and be applied to coated paperboard regardless of the type and morphology of the coating considered. The initial objective to establish a universal correlation was therefore reconsidered in favour of building individual models specific to the nature of the barrier polymer considered.

In the next phase of the study, a correlation between HVTR and specific migration of DiBP and DBP for a PVDC barrier polymer was constructed by varying the applied coating weight. DEHP was excluded as the migration levels detected were below the LOQ. The vapour transport mechanism for the HVTR test and the specific migration test were found to have different dependencies on the coating weight. The HVTR test was found to be independent of coating weight and was rather dependent on the presence of pinholes. The opposite applied to the specific migration of DiBP and DBP where the specific migration was found to be rather independent of pinholes and dependent on the coating weight. This showed that a direct correlation between HVTR and the specific migration was again not possible. However, an indirect correlation could be made. The HVTR method would give an indication of film integrity, whereas the coating weight could be used as an indicator of the specific migration of DiBP and DBP provided the quantity of the chemical contaminant originally

present in the paperboard was known. The correlation between the coating weight and the specific migration yielded an equation that can be used to calculate the specific migration of DiBP and DBP through the PVDC barrier polymer.

The coating weight to specific migration correlation enabled the estimation of the specific migration of DiBP and DBP at the accelerated conditions of 3 days at 60°C. However, it was necessary to relate the estimated specific migration test at 60°C to commercial conditions of use such as packaging for breakfast cereal that is used at room temperature i.e. 23°C. The accelerated migration conditions of 3 days at 60°C was found to correspond to 111 days at 23°C as calculated using the Arrhenius equation. This means that the correlation between coating weight and specific migration at 60°C for 3 days is representative of the efficiency of the functional barrier used for the breakfast cereal packaging for 111 days at the actual conditions of use i.e. 23°C.

The correlation between the coating weight and the specific migration of DiBP and DBP is specific to the type of barrier polymer, the specific chemical contaminant as well as the intended shelf-life of the food product to be packaged in the paperboard. This correlation would enable the estimation of the efficiency of a functional barrier to retard the migration of specific chemical contaminants on a quality control level as well as to estimate whether the product will comply with legal regulations pertaining to food contact packaging.

7.2   Recommendations and future work

The coating weight to specific migration correlation equations should be developed for a wider variety of chemical contaminants such as benzophenones, naphthalenes, and ketones but to name a few. In this study, only three different phthalates were used. A correlation equation could not be established for DEHP because the migration levels observed were below the LOQ. It would be valuable to determine for which of the currently regulated chemical contaminants correlation equations can be established.

Packaging for breakfast cereal used at room temperature i.e. 23°C was used as an example of how the coating weight to specific migration correlation could be used to estimate the migration levels in commercial samples. The accelerated conditions used to establish the correlation only related to 111 days at 23°C, but the shelf-life of breakfast cereal is usually 12 months. In order for the coating weight to specific migration correlation to represent 12 months at 23°C, the accelerated testing time would need to be extended from 3 days to 10 days.

REFERENCES

1. Smook GA. Handbook for Pulp & Paper Technologists. 3rd ed. Vancouver: Angus Wilde Publications Inc.; 2002.

2. Diesen M. Economics of the Pulp and Paper Industry. Finland: Finnish Paper Engineers' Association; 2007.

3. PAMSA. Summary fundings from 2012 production, import and export statistics [4 September 2013]. Available from: http://www.thepaperstory.co.za/wp-content/uploads/2011/09/PAMSA-2012-report_final1.pdf.

4. PRASA. South African Paper Recycling Statistics for 2012 [4 September 2013]. Available from: http://www.thepaperstory.co.za/wp-content/uploads/2011/09/LB344-PRASA-Statistics-2012.pdf.

5. Escabasse JY, Ottenio D. Food - contact paper and board based on recycled fibres: Regulatory aspects - new rules and guidelines Food Additives and Contaminants. 2002;19:79 - 92.

6. Pulp from reclaimed fibre. FDA. 21 CFR 176.260 (1995) Washington DC.

7. Triantafyllou VI, Akrida-Demertzi K, Demertzis PG. A study on the migration of organic pollutants from recycled paperboard packaging materials to solid food matrices. Food Chemistry. 2007;101:1759 - 1768.

8. Aurela B, Kulmala H, Soderhjelm L. Phthalates in paper and board packaging and their migration into Tenax and sugar. Food Additives and Contaminants. 1999;16:571 - 577.

9. Anderson WAC, Castle L. Benzophenone in cartonboard packaging materials and the factors that influence its migration into food. Food Additives and Contaminants. 2003;20(6):607 - 618.

10. Boccacci-Mariani M, Chiacchierini E, Gesumundo C. Potential migration of Diisopropyl naphthalenes from recycled paperboard packaging into dry foods. Food Additives and Contaminants. 1999;16(5):207 - 213.

11. Castle L, Damant AP, Honeybone CA, Johns SM, Jickells SM, Sharman M, et al. Migration studies from paper and board food packaging materials. Part 2. Survey for residues of dialkylamino benzophenone UV-cure ink photoinitiators. Food Additives and Contaminants. 1997;14(1):45-52.

12. Biedermann M, Grob K. Is recycled newspaper suitable for food contact materials? Technical grade mineral oils from printing inks. European Food Research and Technology. 2010;230:785 - 796.

13. Castle L. Migration from recycled paper and board to dry foods. Research into the factors involved, leading to practical avoidance and amelioration measures. York: Food Standards Agency, 2004 September 2004. Report No.: FD 04/07.

14. Paper and board for food contact. BfR recommendation no. XXXVI, 1 June 2013, Germany

15. Industry Guideline for the Complaince of Paper & Board Materials and Articles for Food Contact, Confederation of European Paper Industries (2010).

16. Tiggelman I. Migration of organic contaminants through paper and plastic packaging. Stellenbosch: University of Stellenbosch; 2012.

17. Franz R, Stormer A. Migration of Plastic Constituents. In: Piringer O, Baner AL, editors. Plastic Packaging. Weinheim: Wiley - VCH; 2008.

18. Plastic materials and articles intended to come into contact with food, European Commision Directive 10/2011, 14 January 2011,

19. Gajdos J, Galic K, Kurtanjek Z, Cikovic N. Gas permeability and DSC characteristics of polymers used in food packaging. Polymer Testing. 2001;20:49-57.

20. Siracusa V. Food packaging permeability behaviour: A report. International Journal of Polymer Science. 2012;2012:11.

21. Klopffer MH, Flaconneche B. Transport properties of gases in polymers: Bibliographic review. Oil & Gas Science and Technology. 2001;56(3):223-244.

22. Masaro L, Zhu XX. Physical models of diffusion for polymer solutions, gels and solids. Progress in Polymer Science. 1999;24:1999.

23. Cloete V. Impact of molecular structure on water vapour sorption properties in nanostructured polymeric films. Stellenbosch: University of Stellenbosch; 2011.

24. Crank J, Park GS. Diffusion in polymers. London: Academic Press; 1968.

25. Duda JL, Zielinski JM. Free - Volume Theory. In: Neogi P, editor. Diffusion in Polymers. New York: Marcel Dekker; 1996.

26. Chatham H. Oxygen diffusion barrier porperties of transparent oxide coatings on polymeric substrates. Surface and Coatings Technology. 1996;78:1-9.

27. Prins W, Hermans JJ. Theory of permeation through metal coated polymer films. Journal of Physical Chemistry. 1959;63:716-719.

28. Zulch A, Piringer O. Measurement and modelling of migration from paper and board into foodstuffs and dry food stimulants. Food Additives and Contaminants. 2010;27(9):1306 - 1324.

29. Hauder J, Benz H, Ruter M, Piringer O. The specific diffusion behaviour in paper and migration modelling from recycled board into dry foodstuffs. Food Additives and Contaminants: Part A. 2013;30(3):599-611.

30. Hellen EKO, Ketoja JA, Niskanen KJ, Alava MJ. Diffusion through fibre networks. Journal of Pulp and Paper Science. 2002;28(2):55 - 62.

31. Castle L. Chemical migration into food: an overview. In: Barnes KA, Sinclair CR, Watson DH, editors. Chemical migration and food contact materials. Cambridge, England: Woodhead Publishing Limited; 2007.

32. Nerin C, Contin E, Asensio E. Kinetic migration studies using Porapak as solid - food simulant to assess the safety of paper and board as food - packaging materials. Anal Bioanal Chem. 2007;387:2283 - 2288.

33. Pocas MdF, Oliveira JC, Pereira JR, Brandsch R, Hogg T. Modelling migration from paper into a food simulant. Food Control. 2001;22(2):303 - 312.

34. Triantafyllou VI, Akrida-Demertzi K, Demertzis PG. Determination of partition behaviour of organic surrogates between paperboard packaging materials and air. Journal of Chromatography A. 2005;1077:74 - 79.

35. Tehrany EA, Desobry S. Partition coefficients in food/packaging systems: a review. Food Additives and Contaminants. 2004;21(12):1186 - 1202.

36. Mrkic S, Galic K, Ivankovic M, Hamin S, Cikovic N. Gas transport and thermal characterisation of mono- and di-polyethylene films used for food packaging. Journal of Applied Polymer Science. 2006;99:1590-9.

37. Vollmer A, Biedermann M, Grundbock F, Ingenhoff J-E, Biedermann - Brem S, Altkofer W, et al. Migration of mineral oil from printed paperboard in dry foods: Survey of the German Market. European Food Research and Technology. 2011;232(1):175 - 182.

38. Evaluation of certain food additives: Joint FAO / WHO Expert Committee on Food Additives. Geneva. World Health Organisation; 2002. Report 913(59).

39. Pastorelli S, Sanches-Silva A, Cruz JM, Simoneau C, Losada PP. Study of the migration of benzophenone from printed paperboard packages to cakes through different plastic films. European Food Research and Technology. 2008;227:1585 - 1590.

40. Conditions for determination of migration from paper and board using modified polyethylene oxide (MPPO) as a simulant, DIN EN 14338 (2004).

41. Triantafyllou VI, Akrida-Demertzi K, Demertzis PG. Migration studies from recycled paper packaging materials: Development of an analytical technique. Analytical Chimica Acta. 2002;467:253 - 260.

42. Summerfield W, Cooper I. Investigation of migration from paper and board into food - developement of methods for rapid testing. Food Additives and Contaminants. 2001;18(1):77 - 88.

43.   Pocas MF, Oliveira JC, Pereira JR, Hogg T. Consumer exposure to phthalates from paper packaging: an integrated approach. Food Additives and Contaminants: Part A. 2010;27(10):1451 - 1459.

44.   Al-Fawzan MA. Methods for estimating the parameters of the Weibull distribution. Interstat Statistics on the Internet. October (2000). [4 December 2013]. Available from: http://interstat.statjournals.net/YEAR/2000/articles/0010001.pdf

45.   Dorner WW. Using Microsoft Excel for Weibull Analysis: Quality Digest; 1999 [4 December 2012]. Available from: http://www.qualitydigest.com/jan99/html/body_weibull.html.

46.   Mineral oil contamination of food packed in recycled paper and board: Smithers-Pira 2011 [29 January 2012]. Available from: http://www.smitherspira.com/testing/mineral-oil-contamination-of-food-packed-in-recycled-paper-and-board.aspx.

47.   Ewender J, Franz R, Welle F. Permeation of mineral oil components from cardboard packaging material through polymer films. Packaging Technology and Science. 2012;26(7):423-434.

48.   Fiselier K, Grob K. Barriers against the migration of mineral oil from paperboard food packaging: Experimental determination of breakthrough periods. Packaging Technology and Science. 2012;25(5):285-301.

49.   Biedermann M, Fiselier K, Grob K. Aromatic hydrocarbons of mineral oil origin in foods: Method for determining the total concentration and first results. Journal of Agricultural and Food Chemistry. 2009;57(19):8711 - 8721.

50.   Song YS, Begley T, Paquette K, Komolprasert V. Effectiveness of polypropylene film as a barrier to migration from recycled paperboard packaging to fatty and high moisture food. Food Additives and Contaminants. 2003;20(9):875 - 883.

51.   Gartner S, Balski M, Koch M, Nehls I. Analysis and migration of phthalates in infant food packed in recycled paperboard. J Agric Food Chem. 2009;57:10675 - 10681.

52.   Tiggelman I, Pasch H, Hartman PC. Rapid comparison of mineral oils vapour transmission rate through paper and board packaging materials. Tappi. 2012;11(6).

53.   Diehl H, Seyffer H, Pfeiffer AM, editors. Barrierewirkung ausgewahlter Kunstooffmaterialien gegen die Migration von Mineralolfraktionen in Lebensmittel. BfR Workshop Mineralole in Lebensmittelverpackungen - Entwicklungen und Losungsansatze; 2011 22-23 September 2011; Berlin.

54.   Seyffer H, Cimpeanu CE, Diehl H, inventors; BASF SE, assignee. Paper and cardboard packaging with barrier coating of a polymer mixture. Germany 2012.

55.   MacLeod DM. Wire-wound Rod Coating. In: Satas D, Tracton AA, editors. Coatings Technology Handbook. 2nd ed. New York: Marcel Dekker Inc.; 2001.

56. Booth GL. Rod Coaters. In: Walter JC, editor. The Coating Process. Atlanta: Tappi Press; 1993.

57. Analysis and evaluation of diffusion processes: Fabes Forchungs-GmbH; [19 September 2013]. Available from: http://www.fabes-online.de/migracell.php?lang=en.

58. Aurela B, Tapanila T, Osmonen R, Soderhjelm L. Development of methods for testing barriers in food packaging materials. JHighResolChromatogr. 1997;20(9):499-502.

59. Phthalate hazard assessments [Internet]. NICNAS. 2007 [cited 14 April 2013]. Available from: http://www.nicnas.gov.au/chemical-information/other-assessment-reports/phthalates-hazard-assessment-reports.

60. Atkins P, de_Paula J. Atkins' Physical Chemistry. 7th ed 2001.

61. Choi JO, Jitsunari F, Asakawa F, Park HJ, Lee DS. Migration of surrogate comtaminants in paper and paperboard into water through polyethylene coating layer. Food Additives and Contaminants. 2002;19(12):1200-1206.

62. Ashley RJ. Permeability and plastics packaging. In: Comyn J, editor. Polymer Permeability. England: Elsevier Applied Science Publishers Ltd; 1985.

63. Rogers CE. Permeation of gases and vapours in polymers. In: Comyn J, editor. Polymer Permeability. England: Elsevier Applied Science Publlishers Ltd; 1985.

64. Correlation Coefficient: MathBits.com; [17 October 2013]. Available from: http://mathbits.com/MathBits/TISection/Statistics2/correlation.htm.

65. Stern SA, Trohalaki S. Fundamentals of gas diffusion in rubbery and glassy polymers. In: Koros WJ, editor. Barrier Polymers and Structures. Washington: American Chemical Society; 1990.

66. Weinkauf DH, Paul DR. Effects of structural order on barrier properties. In: Koros WJ, editor. Barrier Polymers and Structures. Washington: American Chemical Society; 1990.

67. Kurek M, Klepic D, Scetar M, Galic K, Valic S, Liu Y, et al. Gas barrier and morphology characteristics of linear low-density polyethylene and two different polypropylene films. Polym Bull. 2001;67:1293-1309.

68. Zheng; Q, Mauro; JC, Smedskjaer; MM, Youngman; RE, Potuzak; M, Yue Y. Glass-forming ability of sode lime borate liquids. Journal of Non-Crystalline Solids. 2012;358:658-665.

69. Weiss J, Leppin CH. Aluminium metallization of polyester and polypropylene films: Properties and transmission electron microscopy microstructure investigations. Thin Solid Films. 1989;174:155-158.